Title
Modeling a Mandibular Functional Shift and the Resulting Temporomandibular Joint Dysfunction in Mice

Permalink
https://escholarship.org/uc/item/7bk27169

Author
Navarro Palacios, Ana Alejandra

Publication Date
2020

Peer reviewed|Thesis/dissertation

Modeling a Mandibular Functional Shift and the Resulting Temporomandibular Joint Dysfunction in Mice

by
Ana Alejandra Navarro Palacios

THESIS
Submitted in partial satisfaction of the requirements for degree of
MASTER OF SCIENCE

in

Oral and Craniofacial Sciences

in the

GRADUATE DIVISION
of the
UNIVERSITY OF CALIFORNIA, SAN FRANCISCO
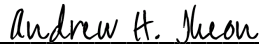
Approved:

DocuSigned by:
_A G_
C84D7533F9714EF...
Alice Goodwin
Chair

DocuSigned by:
Andrew H. Jheon
DocuSigned by: ...CA...
Andrew H. Jheon

DocuSigned by:
Sunil Kapila
A932A5C7F6B145F...
Sunil Kapila

_____

_____
Committee Members

Modeling a Mandibular Functional Shift and the Resulting Temporomandibular Joint Dysfunction in Mice

Ana Alejandra Navarro Palacios

Abstract

The objective of this study was to develop a novel mouse model to evaluate functional adaptation of the temporomandibular joint to malocclusion. We intended to determine the effect of a mandibular functional shift on the size, shape, and symmetry of the craniofacial skeleton utilizing three-dimensional (3D) semi landmarks and geometrics morphometrics (GM) as well as to analyze histologically the cellular and molecular changes in the temporomandibular joint (TMJ) and in the mandibular condylar cartilage (MCC). A mouse model of a mandibular functional shift was created by extracting 3 molars from the maxillary right quadrant in FVB/NJ wildtype mice. Teeth were extracted at 3 weeks old, and samples were collected at 6 weeks so that mice developed a functional shift during a maximal growth period from weaning to sexual maturity. The experimental group consisted of 11 mice (5 females and 6 males), and the control group was composed of 10 mice (4 females and 6 males). Micro CT (μCT) was performed on the entire heads of experimental and control mice. The TMJs on both the extraction and non-extraction sides in the experimental animals were compared to the control (with no teeth extracted) for the following variables: (1) geometric morphometric analysis of the size and shape of craniofacial skeleton, including the cranium, cranial base, maxilla, and mandible; (2) changes in bone volume and density of the TMJ condyle were determined using the μCT data, and (3) the TMJ and MCC were analyzed histologically and by *in situ* hybridization for specific markers. Overall, the size and shape of the cranial skeleton was not affected in the extraction model; however, there were changes in the mandibular shape. In the

mandible, the molar alveolus height was increased on the extraction side compared to non-extraction and control. The condylar head and neck width were narrower, and the superior surface of the condylar head was more convex on both the extraction side and the non-extraction side in the experimental animals compared tocontrols. Furthermore, the bone volume of the condylar process on both the extraction side and the non-extraction side in the experimental animals was decreased by 15%, and the bone density was increased by 5% compared to condyles from control animals. Finally, the MCC was thinner in both the extraction and non-extraction sides in the experimental group, and the expression of *Col2* and *Col10* was increased, suggesting an expansion in maturation stage and hypertrophic chondrocytes, and there was ectopic expression of *Col1* in the MCC, suggesting a pro-osteogenic response in the extraction condyle samples compared to controls.

Our results suggest extraction of the molars in one quadrant in our mouse model resulted in a presumed shift in the mandible and degenerative adaptations in the condylar shape. There was loss of bone volume in the condylar process and apparent deposition of bone with increased mineral density near the condylar head surface in both condyles of the extraction mice compared to controls. At the cellular level, there was an increase in maturation stage and hypertrophic chondrocytes and osteoblasts in the MCC that may have contributed to the remodeling and bone deposition at the condylar surface. This phenotype is suggestive of osteoarthritic changes in that thinning of the MCC and increased bone deposition at the condylar surface was observed. These data further elucidate the tissue and cellular changes in the condyle due to a functional shift, which furthers our understanding of the pathology of this malocclusion.

Table of Contents

Introduction

Central Hypothesis

Specific Aims

Materials and Methods

Results

Discussion

Conclusion

References

List of Figures

Figure 1.

Extraction of maxillary right molars results in significant changes in mandibular

Figure 2.

Extraction of maxillary right molars alters the shape of the condylar processes

Figure 3.

The condylar processes in the extraction model have decreased bone volume and

Figure 4.

The mandibular condylar cartilage is thinner, and chondrocytes appear compacted in

Figure 5.

The mandibular condylar cartilage is thinner in extraction condyle compared to

Figure 6.

There is decreased apoptosis in the non-extraction side condyle compared to the

List of Tables

Introduction

Structure and development of the mammalian temporomandibular joint

The temporomandibular joint (TMJ) is a complex skeletal structure that is essential for jaw movement in mammals. It is a ginglymoarthrodial joint, meaning a joint that is able to perform both rotational and translational movements (Purcell et al. 2009). The TMJ is composed of the mandibular condyle that fits into the mandibular fossa of the temporal bone of the skull. Separating these two bones from direct contact is the articular disc. The morphology of the disc matches the condylar head and the mandibular fossa. In the frontal view, the disc is concave inferiorly, designed to fit over the condylar head and convex superiorly to fit the concave surface of the mandibular fossa of the temporal bone (Laskin et al. 2006). In the sagittal plane, it can be divided into three regions according to thickness. The central area is the thinnest while the anterior and posterior regions are much thicker in comparison. From the anterior view, the disc is thicker medially than laterally. The articular portion of the disc is comprised of dense fibrous connective tissue devoid of any nerves and vessels while the posterior attachment of the disc is innervated and richly vascularized. The fibrocartilaginous articular disc divides the joint cavity into two compartments, and specific tendons and muscles are associated with each compartment (Li et al. 2014; Owtad et al. 2013). Furthermore, the tendons of the pterygoid muscle and various surrounding ligaments are associated with the TMJ (Bravetti et al. 2004). The disc is attached to the condyle both medially and laterally by collateral ligaments. The articular disc is attached posteriorly to a region of loose connective tissue, known as retrodiscal tissue, which is innervated and highly vascularized. Rotational movement occurs between the condyle and the inferior surface of the disc during early

1

opening, and translation takes place in the space between the superior surface of the disc and the fossa during lateral opening. Synovial fluid facilitates movement within the joint; it also serves as a medium for the transportation of nutrients and waste products from the articular surfaces of the condyle and glenoid fossa (Soydan et al. 2014).

The embryonic development of the TMJ is similar across various mammalian species, including mice and humans, however, it differs significantly from that of other synovial joints (Li et al. 2015). In contrast to the formation of long bone joints by cleavage or segmentation within a single skeletal condensation, the TMJ develops from two distinct and widely separated mesenchymal condensations: the glenoid fossa blastema and the condylar blastema (Li et al. 2014). The glenoid fossa blastema is derived from the otic capsule and undergoes intramembranous ossification (Wang et al. 2011; Gu et al. 2008). The condylar blastema develops towards a rectangular cell condensation located lateral and superior to Meckel's cartilage, and it is subsequently attached medially by the lateral pterygoid muscle as a result of rapid cellular proliferation (Bravetti et al. 2004). Simultaneously, the condylar blastema develops from the secondary condyle cartilage of the mandible and forms bone via endochondral ossification, subsequently extending in an anterior/medial direction and capping the condylar blastema (Merida et al. 2009; Yokohama-Tamaki et al. 2011).

The mesenchyme between the glenoid fossa and condylar blastemas condenses, prior to the separation of the two primordia of the TMJ, to form an articular disc (Wu et al. 2014). As the condyle develops continuously upward approaching the glenoid fossa, the mesenchyme differentiates into layers of fibrous tissue, ultimately separating the upper and lower synovial cavities in a process termed cavitation (Gu et al. 2014). Via cellular

processes of proliferation and differentiation, the condyle anlage is configured into a typical secondary cartilage and superficially covered with a thick layer of flat fibrous cells (Vinkka-Puhakka et at. 1993; Kenzaki et al. 2011). The glenoid fossa exhibits intramembranous ossification, which occurs at the same time as condylar differentiation (Wang et al. 2011). During the development of the skeletal elements of the TMJ, morphogenesis of the soft tissues surrounding the joint continues. Following the completion of cavitation, the TMJ exhibits marked ossification and growth of the condyle and glenoid fossa, functional remodeling of the articular disc via an avascular event, and substantial condensation (Owtad et al. 2011). Furthermore, bones of the joint and the articular disc are encapsulated by the joint capsule, and the development of the muscles and ligaments associated with the joint proceeds (Liu et al. 2013; Ricks et al. 2013). Although the structure and function of the TMJ has been well characterized, the molecular and cellular mechanisms underlying its formation and development remain unclear.

Mandibular condylar cartilage

The mandibular condylar cartilage (MCC) is unique in that it is a secondary cartilage, meaning that it develops after bone, while primary cartilage in limbs is replaced by bone, and secondary cartilage remains cartilage throughout the life of the animal. The major role of the MCC is to support and distribute functional loads, allowing for frictionless motion and prevention of the breakdown of the cartilage (Orajarvi et al. 2018). In addition, the MCC acts as a site of growth for the mandible, thus, acting as a growth plate and articular cartilage in one, unlike in other joints in which the growth plate and articular

surface are separated, and the epiphysis (growth plate) fuses upon the completion of growth.

Although it does not develop an epiphysis, the MCC is organized in a growth plate-like structure that is subdivided along its main axis into four distinct layers. Interestingly, the MCC is composed of cells only partially differentiated along the chondrogenic pathway which are alkaline phosphatase positive and express type I and type II collagen, suggesting they may differentiate into chondrocytes or osteoblasts. The MCC is a fibrocartilage, and unlike hyaline cartilage, expresses type I collagen. The most superficial layer is called the articular or superficial zone; it forms the outermost functional surface, and it is found adjacent to the to the joint cavity. This zone is responsible for dissipating shearing and frictional loads generated by jaw functions, and it expresses superficial zone protein (SZP) which is a large proteoglycan that is synthesized and secreted into synovial fluid. SZP is known to function as a boundary lubricant by reducing the coefficient of friction of the MCC surface and the strain energy of the synovial fluid (Ohno et al. 2006; Jay et al. 2007). The second layer is the polymorphic (PM) progenitor cell zone. This zone is mainly cellular with undifferentiated mesenchymal tissue. The cartilage cells in this zone are large and enclosed in lacunae. There is no organization of formation or arrangement of chondrocytes in this zone. This tissue is responsible for the proliferation of articular cartilage in response to the functional demands placed on the articular surface during loading and unloading. This zone is characterized by the expression of *Sox9* and the absence of the expression of *Col2*. The third layer is the flattened chondrocyte (FC) zone. The cartilage cells in this region are highly mature, yet these cells have not lost their ability to proliferate. In this zone, the collagen fibrils are arranged in bundles in a

4

crossing pattern. The cartilage shows a random orientation, providing resistance against compressive and lateral forces. Cells in this zone are characterized by the expression of *Sox9*, Indian hedgehog (*Ihh*), *Col1*, and *Col2*. The fourth and deepest layer is the hypertrophic chondrocyte (HC) zone. In this zone the chondrocytes become hypertrophic, undergo cell death, and have their cytoplasm evacuated, forming bone within the medullary cavity. Cartilage breakdown occurs and cartilaginous spicules undergo calcification with hydroxyapatite crystals. The surface of the extracellular matrix scaffolding provides an active site for remodeling activity as endosteal bone growth proceeds. The bony trabeculae are arranged randomly and not perpendicular to the articulating surface. Cells in this zone are characterized by the expression of *Spp1* (encoding osteopontin), *Ihh*, and *Col10*. It is well known that the extracellular matrix (ECM) surrounding the chondrocytes, which undergoes adaptive remodeling with mechanical stimulation, is the most abundant component of cartilage and can endow the cartilage with the unique capacity to bear load and resist compression (Shibukawa et al. 2007).

We have learned a great deal about the genes involved in TMJ development utilizing mouse models. For example, *Runx2* and *Sox9* are necessary for the development of the MCC since the MCC does not develop in mice with deletion of these genes (Shibata et. al 2004, Mori-Akiyama 2003). Mice with deletion of *Foxc1* have sygnathia and bifurcated condyle and do not develop a disk or glenoid fossa (Inman et al. 2013), and mice lacking *Alk2* present with complete TMJ agenesis (Dudas et al. 2004), suggesting a role for these genes in TMJ development. The MCC is underdeveloped, and the TMJ disc does not form in mice deficient in Ihh (Shibukawa et al. 2007). Thus, mouse

studies have shed light on genes involved in TMJ development; however, more work is necessary to fully understand the signaling involved in the development and maintenance of the TMJ and MCC and ultimately identify therapeutic targets for clinical interventions, such as treatment of TMJ disorders.

Posterior crossbite and functional shift

Posterior crossbite is defined as a reverse occlusion, in which at least one mandibular posterior tooth from canine to molar occludes outside of the maxillary teeth. In patients with unilateral crossbite, the mandible often shifts toward the crossbite side when teeth occlude from rest to the intercuspal position, which is termed a mandibular functional shift (MFS). In some cases, the mandible remains deviated to the crossbite side at rest. Unilateral crossbite is a malocclusion encountered frequently in the orthodontic clinic with a prevalence ranging from 2.7% to 23.3% (Servert et al. 1997; Nerder et al. 1999; Ishizaki et al. 2010; Bishara et al. 1994; Proffit 1991). MFS is a common condition among this patient population since it has a prevalence of 80% to 90% in this group of patients with posterior crossbite (Kutin et al. 1969; Kurol et al. 1992). Clinically, MFS is characterized by facial asymmetry and dental midline discrepancy. It has been suggested that uncorrected mandibular functional shift in growing patients disrupts neuromuscular patterns and alters growth of the mandible, particularly in the condylar region (McNamara 1975). Accordingly, MFS in a unilateral posterior crossbite patient may lead to asymmetrical condylar growth and thus, potentially result in the development of facial asymmetry, which can only be treated surgically in adolescence or adulthood (Sato et al. 1989; Epker et al. 1999).

6

Despite the potentially challenging outcomes of MFS, posterior crossbites can be corrected with expansion of the palatal suture in growing patients in primary or mixed dentition. Since only 10% of posterior crossbites identified in the primary dentition will self-correct during the transition to the mixed dentition (Dimburg et al 2013), it is important to diagnose and treat this malocclusion early, during the primary or mixed dentition stage. Petren et al., (2003), in a systematic meta-analysis of published articles between 1966 and 2002 on early treatment of posterior crossbites, concluded that primary and early mixed dentition intervention has a very high success rate using various fixed and removable maxillary expansion appliances. Fixed lingual archwire designs had 90-100% reported success rates in the correction of posterior crossbites during primary and mixed dentitions. Fixed maxillary jackscrew appliances were reported at close to 100% success rates in the correction of posterior crossbites during the primary and mixed dentitions. Removable splint-acrylic type appliances had somewhat lower success rate at 60-70% in both primary and mixed dentitions (Petren et al. 2003). Thus, there are many effective treatment modalities for posterior crossbite and MFS, and it is important to diagnose and treat in the primary or mixed dentition in order to avoid the development of asymmetry during adolescence and adulthood.

How posterior crossbite and MFS affect growth in patients at the tissue and cellular level is not well understood. Furthermore, the shift results in the condyle on the side opposite the direction of the shift to be displaced anteriorly, or protruded, while the condyle on the side toward the shift is more stable positionally and is likely to be slightly retruded (Fuentes et al 2003; Nakano et al. 2004). How the altered position of the condyle affects the shape and function of the TMJ in patients is not fully understood.

There is some evidence showing the effect of posterior crossbite and MFS on mandibular growth and the TMJ in various animal studies. A number of animal studies suggest that proliferation and growth in the MCC is altered after a change in the postural position of the mandible using intraoral positioners designed to shift the mandibular postural position asymmetrically (Fuentes et al. 2003; Takenobu et al. 2008), maxillary occlusal splints to shift the mandible laterally during closure (Nakano et al. 2004), and grinding mandibular and maxillary molars to create a lateral shift (Poileka et al. 1997; Poileka et al.2000). According to these reports, growth of the MCC adapts to its local functional-biomechanical environment and differential changes in the MCC occur on the non-protruded and protruded sides. Yotsuya et al., (2020) evaluated the role of mechanical loading in the progression of TMJ osteoarthritis in surgical instability arising from unilateral partial discectomy (UPD) in a murine model. They found that on the side where the UPD was performed, late-stage degeneration of the cartilage showed a significant reduction with diminished fibrillation and erosion of the articular cartilage, cell clustering, and hypocellularity, suggesting that select and specific late-stage changes in TMJ osteoarthritis were likely due to the changes in local mechanical environment on the joint (Yotsuya et al 2020). Studies in rats have also shown that inducing a lateral shift using inclined crowns cemented on the maxillary incisors results in changes in growth of condylar head and in trabecular structure and mineralization of the condylar bone (Nakano et al. 2003).

Clinically, unilateral posterior crossbite and MFS can result in asymmetric growth of the mandible and alterations in the MCC in patients, which has been further supported by studies of mouse models with altered occlusion. However, how mandibular growth is

affected is not well understood, and furthermore, very little is known about the effect on shape and function of the TMJ and the molecular response of the MCC as a result of alteration in the habitual position of the mandible.

Geometric morphometrics and its use in orthodontics

Technological advances have made three dimensional orthodontic diagnostic tools much more accessible in the last several decades. We now have 3D images of the craniofacial skeleton from CBCT imaging, dental casts from intraoral and standard scanners, and 3D facial photographs from stereophotogrammetry camera sets, all available in digital format. We are, therefore, in the position to measure and evaluate what interests us most as orthodontists, namely facial shape, in ways that were not possible in the past (Klingerberg et al 2010; Polychronis et al 2013). Potentially, it is a turning point in orthodontic diagnosis. Since 3D data are not a mere extension of 2D data to an extra dimension but require new tools to fully exploit their 3D nature, we can now take this opportunity to improve our diagnostic tools.

Geometric morphometrics (GM) combines geometry, multivariate morphometrics, computer science, and imaging techniques for a powerful and accurate study of organismal forms (Cardini et al. 2013). GM has been traditionally applied to the field of biology to study developmental differences between species (Klingerberg, 2010). Morphometrics is defined as a branch of biology that deals with the characterization of organismal form and quantification of morphological variation. It is derived from the Greek word which means measuring form. Morphometrics is used to quantify the morphological structure of organisms and then present and explain the shape differences.

Geometric morphometrics principles

GM is a special method to measure shape as it does not use traditional angles and linear distances. By selecting specific angles or linear measurements, we arbitrarily choose which part of the shape to measure. In fact, the selection of some measurements and exclusion of others can lead to biased results as you consider just one specific part of the shape rather than the whole of it. With GM, the whole of the shape can be analyzed. The following are basic principles of GM:

1) An object is a collection of landmarks. Objects such as bones and faces need to be reduced to a set of landmarks before analysis can proceed, as the basic tools of GM cannot work directly on curves or surfaces. Objects of the same class (e.g. faces) must have the same number of landmarks, and these have to be homologous (e.g. each landmark must represent the same anatomical or functional feature).

2) Shape of an object can be measured only in relation to another object (e.g. shape measurement is actually the comparison between two measurements of shape difference).

3) The "shape" is the morphologic entity that remains after position and size differences have been removed from the analyzed objects (as dimensional differences are not considered when comparing shapes).

When analyzing a collection of objects, the main purpose is to find the average shape of the objects and then analyze the variability of shape in the group with regard to the average shape. The variability is analyzed through Principal Component

Analysis (PCA). In a biological system, such as the craniofacial complex, shape variability can be translated into shape patterns. GM can reveal these patterns and measure the relative contribution of each to the total shape variability (Webster et al. 2010; Bookstein et al. 1997; Mitteroecker et al. 2009).

From Cartesian coordinates to the shape-space system

The procedure that GM follows to compute average shape and shape variability is a sequence of the following actions:

1) Landmarks are placed on the objects at homologous positions. When all landmarks are placed, we can call the group of landmarks that describe an object as a landmark configuration.

2) The landmark configurations are aligned and scaled using best-fit procedures that minimize differences between them. This step is called Procrustes superimposition. After Procrustes superimposition, we lose all information about size, and we deal only with shape.

3) The Cartesian coordinates (x,y,z) of the scaled/aligned objects are called Procrustes coordinates. The Procrustes coordinates of an object define its position in a system known as shape-space.

4) The shape-space extends along many dimensions since each object has many landmarks. For 3D objects, the number of dimensions of the shape-space is equal to three times the number of landmarks minus seven (degrees of freedom).

5) Each object can be considered as a single point in shape-space. The distance between two objects in shape-space is equal to their shape difference.

6) The average shape of all the objects is the shape at the center of the shape-space and can be easily computed by averaging the Procrustes coordinates of each landmark.

7) To determine the shape patterns of the population, the shape-space is rotated in such a way that is main axes are aligned with the direction of major variability of the population. This is achieved by applying PCA. PCA describes differences between shapes through determination of the main sources of variability when comparing different shapes (Bookstein et al. 1997).

Landmark identification and placement

GM is based on landmark data. A morphological landmark is defined as a point that can be located precisely on each specimen under study and clearly correspond in a one-to-one manner from specimen to specimen (Drydent et al. 2002). When applying GM to objects of interest, such as bone surfaces, we cannot study curves and surfaces directly, but we need to place landmarks on them. Thus, a challenging problem in GM is determining how many landmarks to place, where to place the landmarks, how densely to cover each surface with landmarks, and finally how to confirm that landmarks are homologous from one object to another. This last question is particularly important since in orthodontics we come across some extensive areas that do not possess any distinguishing/non-ambiguous markers. To manage this problem Bookstein developed a classification based on anatomical and geometric criteria and proposed three different

types of landmarks:

1- Type I landmarks are those that are located at the juxtaposition of anatomical features, such as the confluence of three structures meeting at one point. These landmarks are defined by features in their immediate vicinity and can be confidently assumed homologous at least in anatomical sense (e.g., Nasion: the most anterior point of the frontonasal suture on the curve at the bridge of the nose).

2-Type II landmarks are defined as the maximal curvature of an anatomical structure (e.g., the anterior nasal spine defined as the point of the highest curvature of the maxillary outline).

3-Type III landmarks are defined as points along a curve or surface, in relation to some other more distant structure. For example, the menton is located on the mandibular outline but needs other structures (e.g., the Frankfurt horizontal) or an external vertical direction (e.g., the true vertical) to define its precise location (Bookstein 1997a; Bookstein 1997b).

Landmarks should cover the entire structure under study in as regularly placed intervals as possible so that all changes can be detected. Removal of one landmark may alter the entire result. On the other hand, too many landmarks may not provide relevant information about variation in the whole structure.

Curves or surfaces that do not provide explicit information for precise location of landmarks are ubiquitous. The simple solution is to place landmarks at predetermined intervals along the curve. Points placed with such criteria that stay on the curve/surface are called semi-landmarks. The geometry is easier for curves in 2D than 3D, but it is not so easy to define semi-landmarks since placement is not guaranteed to be 100%

homologous. Semi-landmarks are placed in the appropriate position and density until the additional shape variability is reduced to the minimum possible. This is achieved by sliding the semi-landmarks in the direction that reduces shape variance while always constraining them on the curve or surface. Once in the position, the semi-landmarks can be considered homologous points, and the shapes are ready to be analyzed by PCA (Mitteroecker et at. 2009; Gunz et al. 2005).

Advantages and disadvantages of GM

When using GM, we remove any information on size since all the shapes are "averaged", and size information is left out of the Procrustes space. This fact can be seen as a disadvantage as only change in shape patterns can be analyzed through GM. However, this limitation may also be considered an advantage. There is no need to arbitrarily select a special part of the shape to measure as all parts can be compared as long as landmarks fit the area. Another important aspect is that in orthodontics we usually compare anatomical features between patients and controls, assuming that controls are "normal". However, what can be considered normal or not normal is controversial and difficult to determine. With GM, variation in shape is determined from the population in an unbiased manner. Variability analysis via PCA allows us to determine shape patterns and can therefore dictate which measures are important in defining the shape.

Applications of geometric morphometrics in orthodontics

Recently, GM has been widely used in medical fields, as well as orthodontics since orthodontics is focused on the size and shape of the face and its components.

Widespread use of 3D imaging modalities has generated extensive and large volumes of data. Tools for interpreting and organizing these data have not kept pace with the development of more sophisticated imaging. Craniofacial research increasingly utilizes aspects of these data to answer complex questions. While several tools have been used to measure size, proportions, and relationships between anatomical components, shape has been mainly described by esthetic criteria. GM can be used as a specific tool to analyze shape variation between individuals and to identify patterns of variation of orthodontic interest as well as quantify shape-related changes of skeletal tissues in disease and understand the variation in facial morphology in large populations in 3D, which is more accurate than the traditional application of points and lines for measurement in 2D (Guyomarch'h et al. 2014).

During the last century, most research done in orthodontics was based on conventional 2D images and cephalometric analysis. This method is user-friendly and simple which explains why it continues to be in routine clinical use. One of the key advantages of CBCT over 2D radiographs is its ability to provide 3D volume, surface, and sectional information about the craniofacial structures. CBCT has provided orthodontists and researches the ability to overcome the substantial limitations of 2D radiographs, including geometric distortions and superimposed structures (Kapila et al. 2015). Unlike 2D superimpositions provided by conventional cephalometric radiography, CT/CBCT images can provide sophisticated 3D superimpositions and treatment assessment when necessary (Cevidanes et al. 2006).

Translation of methodology developed in two dimensions to three is not straightforward and involves many additional challenges. Traditional use of lines and

cephalometric analysis is inadequate as it does not provide an accurate or complete description of the morphology or the covariation of related structures in 3D. The good news is that methods for statistical shape analysis, such as PCA, are readily applicable to landmarked 3D data sets to classify morphology (Solem, 2017). This explains why the use of GM is a powerful tool to study shape and growth differences, and its use has increased in popularity during the last decade.

More recent orthodontic studies published in the last 20 years have used GM for their data analysis. For example, McIntyre in 2003 described the advantages and disadvantages of GM, its utility in orthodontics, and how it can overcome conventional cephalometric analysis deficiencies (McIntyre et al. 2003). Ghislanzoni et al. in 2017 described how to measure 3D shape in orthodontics using GM, providing a workflow and explaining how to apply this new method as part of the routine orthodontic diagnosis (Ghislanzoni et al. 2017). Pan and his colleagues evaluated deformations that contribute to Class III mandibular configuration employing GM analysis. They found that the thin plate spline (TPS) analysis revealed an anteroposterior elongation of the mandible, which leads to the appearance of a concave profile with a prognathic mandible (Pan et al. 2006). In 2016 Freudenthaler et al. evaluated the role of craniofacial shape in malocclusion by applying GM to a set of two dimensional landmarks and semi-landmarks obtained from lateral skull radiographs. This research group found that craniofacial shape was clearly associated with dental malocclusion and showed considerable variation (Freudenthaler et al. 2017). Tessler et al. compared craniofacial differences between twins discordant for surgically repaired unilateral cleft lip and palate (UCLP) at multiple developmental stages, testing the effect of zygosity on the shape and size of the craniofacial skeleton by means

of TPS analysis. They found that GM showed that surgically repaired UCLP does not produce significant shape or size differences in the craniofacial features of monozygotic or dizygotic twins discordant for UCLP (Tessler et al. 2011). Latif and his colleagues compared facial morphology in subjects with unrepaired complete bilateral clefts and unaffected controls using GM. PCA showed that facial variation in subjects with clefts occurred in the anteroposterior direction, whereas in controls it was mostly in the vertical direction. These differences in the direction of facial variability suggest that individuals with bilateral clefts can have an intrinsic growth impairment affecting facial morphology later in life (Latif et al. 2020).

Finally, Chang et al. studied the cranial base morphology of Asians and its relationship with class III malocclusion due to mandibular prognathism. This group tested the hypothesis that developmental heterogeneity in cranial base morphology increases prevalence of class III malocclusion and mandibular prognathism in Asians. TPS analysis of lateral cephalograms of the cranial base and the upper midface configuration were compared between one European-American group and four Asian ethnic groups of young adults with clinically acceptable occlusion and facial profiles. TPS analysis showed that the greatest differences in the Asian populations were the horizontal compression and vertical expansion in the anterior portion of the cranial base and upper midface region. The most posterior cranial base region also showed horizontal compression between the basion and Bolton point with forward displacement of articulare. Facial flatness and anterior displacement of the temporomandibular joint resulted in a relative retrusion of the nasomaxillary complex and relative forward position of the mandible. These features that tend to cause prognathic mandible and/or retruded midface indicated a morphologic

predisposition of Asian populations for class III malocclusion (Chang et al. 2014).

Central Hypothesis

Inducing a functional shift in our mouse model by extracting molars in the maxillary right quadrant will result in changes in the shape of the mandible, in particular the condyle, differences in bone volume and density of the condylar head, and degeneration of the MCC, including disorganization and alterations in the chondrocyte populations in the MCC compared to control.

Specific Aims

Aim 1: To determine the effect of a mandibular functional shift on the size, shape, and symmetry of the craniofacial skeleton in an extraction mouse model. *I hypothesize that inducing a functional shift in our mouse model by extracting molars in the maxillary right quadrant will result in asymmetric growth of the craniofacial skeleton, including changes in the shape of the mandible compared to control.* We will perform geometric morphometric analysis on the complete skull, including the maxilla, mandible, and cranium, of experimental and control mice. We will also analyze the bone volume and density of the condylar processes. The analysis proposed in Aim 1 will show whether a mandibular functional shift during growth does indeed affect the shape of the cranial skeleton, in particular the mandible, and bone volume and density in a mouse model.

Aim 2: To analyze the histologic cellular and molecular changes in the temporomandibular joint (TMJ) and mandibular condylar cartilage (MCC) in a mandibular functional shift mouse model. *I hypothesize that a mandibular functional shift in our extraction mouse model will result in degeneration of the MCC, including disorganization and alterations in the chondrocyte populations in the MCC, decreased chondrocyte proliferation and increased cell death in the MCC, and alterations in osteoblast and osteoclast activity in the MCC on the experimental side.* In Aim 2, I will analyze (1) the gross changes in MCC thickness, (2) changes in cell morphology and organization, (3) differences in cell proliferation and death, and (4) osteoblast and osteoclast markers in the MCC in the experimental and control mice.

Materials and Methods

Animals:

FVB/NJ mice from Jax Lab were utilized for the experiments in this study. At 3 weeks of age, all 3 molars from the maxillary right quadrant were extracted under anesthesia with ketamine and xylazine in the experimental mice. Experimental and control littermates with no teeth extracted were euthanized and mouse heads were collected at 6 weeks old. The experimental group consisted of 11 mice (5 females and 6 males), and the control group was composed of 10 mice (4 females and 6 males). For the morphometric analysis of the skull, the scan for one of the experimental female skulls was distorted, and so only 10 experimental mice (4 females and 6 males) were analyzed. All animal procedures were performed following approval from the Institutional Animal Care and Use Committee.

Micro-computed tomography:

Micro-computed tomography (μCT) was performed on the entire skull of the experimental and control mice. 6 week-old experimental and control mice were collected, and the heads were removed, fixed in 4% paraformaldehyde (PFA), and dehydrated in 70% ethanol. Samples were scanned with the SF VA Medical Center Bone Imaging Core Facility using a MicroCT50 (Scanco Medical), 55kVp, 109μA, 6W. Heads were scanned at 20μm voxel size, with a 500ms integration time and a 20.5mm field of view. The number of slices per sample was 600. The scanner was calibrated for bone using an AL 0.5m filter calibrated to 55kVp, 0.5mm AI, BH: 1200mg HA/ccm, scaling 4096. 3D image processing and analysis was carried out using Avizo Lite software (version 9.1.1, Thermo

Fisher Scientific). Bone volume and density were calculated according to grayscale intensity using the Material Statistics module of Avizo 9.1.1.

Geometric morphometric analysis:

µCT data was imported into Avizo Lite (version 9.1.1, Thermo Fisher Scientific), where the craniums and mandibles were manually separated. Using consistent thresholds, isosurfaces were generated for each anatomical region. Isosurfaces were brought into Landmark (Institute for Data Analysis and Visualization) where the cranium, mandible, and condyles were landmarked. Three landmark schemes were utilized: scheme one included 44 landmarks to capture the cranium morphology (Supplemental Figure 1) (Hill et al. 2009); scheme two consisted of 26 bilateral landmarks for the mandibles (Figure 1B) (Hassan et al. 2019); and set three included four arrays of 40 sliding semi-landmarks designed to recapitulate the structure of the condylar processes (Figure 2A), and the arrays were placed on the medial and distal sides of each condyle (Figure 2A'). For the semi-landmarking, each array included 9 landmarks (Figure 2A') which bounded the equidistantly placed semi-landmarks. The landmark coordinates were exported as text files and imported into MorphoJ (Version 2, Apache License, Klingenberg, C.P. 2011) (Klingenberg et al. 2011) for statistical evaluation of shape differences. Centroid size, defined as the square root of the sum of squared deviations of landmarks from their centroid, was examined between control and experimental groups for each anatomical region using a Student's T-Test; no significant differences were found. To eliminate orientation, size, and position, a Procrustes superimposition was performed on the landmark data. To examine the major differences in shape between the

22

control and extraction groups, a principal component analysis (PCA) was conducted. PCA is a method that preserves information while simplifying higher dimensional data into mutually orthogonal dimensions called principal components. Wireframes of the maximum, average, and minimum shape variants were generated to visualize the full spectrum of shape variation recapitulated by a principal component. Canonical variate analysis (CVA) or a linear discriminant analysis (for this data) was also performed for each anatomical region between control and extraction groups. CVA is a method of multivariate analysis designed to maximally separate predefined groups based off of their intragroup variation. From this analysis, the Procrustes and Mahalanobis distances among groups were found and permutation (10,000 permutations) tests were conducted to generate p-values.

Histological analysis:

Heads were collected from experimental and control animals, fixed in 4% paraformaldehyde overnight at 4°C, demineralized in EDTA (0.5M) for 1 week, paraffin processed and embedded, and sectioned at 7µM on a Leica microtome in order to perform histological analysis of the TMJ and MCC. Hematoxylin and eosin (H&E) and safranin O staining was performed on sections following standard protocols. To assess cell death, TUNEL staining (In Situ Cell Death Detection Kit, TMR red, Roche 12156792910) was performed following kit protocols, and TUNEL positive cells were imaged and quantified. RNAscope (ACD Diagnostics), an *in situ* hybridization assay for detection of target RNA within intact cells, was performed following standard manufacturers protocols with specific mouse probes against *Col1a1* (#537048), *Col2*

(#407228), *Col10* (#426181), and *Mmp13* (#427601). Sections were imaged on a DMi8

upright microscope.

Results

Extraction of molars in the maxillary right quadrant resulted in changes in the shape of the mandible and condyle.

The experimental design of the project was to extract the three molars from the maxillary right quadrant of mice at postnatal day (P) 21 at the time of weaning, when the molars are just erupting (Figure 1A). We then allowed the mice to develop normally until P42 or six weeks when the mice reach sexual maturity and then euthanized both the experimental mice with teeth extracted and control littermates with no tooth extractions. Heads were μCT scanned, isosurfaces were generated and landmarked (landmarks for mandible shown in Figure 1B, condyle Figure 2A', and cranium Supplemental Figure 1), and geometric morphometric analysis was performed on the skull (cranium, cranial base, and maxilla), mandible, and condylar head.

Procrustes superimposition was completed, and no significant difference in centroid size of the skulls between the control and extraction groups was noted, and so there was no need to account for size difference in the data (Supplemental Table 1). To investigate the role of sex in our data, canonical variate analysis (CVA) was executed on all anatomical regions of interest and delineated by sex. For every region, the Procrustes distance was calculated between males and females, and no statistically significant differences were found (Supplemental Table 1). PCA was also performed comparing the control and experimental samples by sex, and it clearly illustrated that the data clustered by experimental group and not sex (Supplemental Figure 2).

We observed significant changes in the shape of the mandible after extraction of maxillary right molars (Supplemental Table 1). Overall, the control and extraction groups separated completely, and the majority of the variation between the groups was accounted for by principal component (PC) 1 (41.84%) and PC2 (13.44%; Figure 1C, Supplemental Table 2). CVA was also performed and showed clear separation between experimental and control samples (Supplemental Figure 3A).

A major difference in the mandibular body shape was the height of the alveolar bone which was significantly increased in the right (extraction side) mandible compared to the left (non-extraction side) mandible of the extraction mice or control mice. Due to the extraction of the maxillary right molars on the right side, there was compensatory eruption of the opposing mandibular molars on the right, as expected, and so the molars hyper-erupted as seen in the wireframe and isosurface images (Figure 1D, D'). Linear measurements also showed a significant difference in the alveolar height of the right mandible and not of the left mandible in the experimental mice compared to control (Supplemental Figure 4). Otherwise, the shape of the right (extraction) and left (non-extraction) mandibles were fairly similar, when comparing both sides together (Figure 1C-D').

When we compare the right (extraction side) mandible to control only, we see separation of control and extraction samples along PC1 (46.67%) and PC2 (17.02%; Figure 1E, Supplemental Table 2). There were significant shape differences in the right extraction mandible compared to control (Supplemental Table 1, Supplemental Figure 3B) as shown by the PC1 Max in the wireframe (Figure 1F) and isosurface (Figure 1F') including, as mentioned the increase in alveolar bone height, increased height at the

lower border of the mandible, decreased length of the angular process, and increased posterior-inferior tip of the condylar process. The left, non-extraction side mandible also separated significantly from the control (Supplemental Table 1, Supplemental Figure 3C) along PC1 (47.01%) and PC2 (13.24%; Figure 1G, Supplemental Table 2), and there were similar differences in the shape of the lower border of the mandible, angular process, and condylar process compared to control (Figure 1H, H'). Thus, interestingly, although the extraction was only done on the right hemi-mandible, we observed changes in the mandibular shape in both the right and left hemi-mandibles compared to control.

The isosurfaces of the right and left mandibles in the extraction mice showed significant changes in the condylar head that were not entirely captured by the mandibular landmarks (Figure 1F', H'). In order to more precisely measure the changes in shape of the condylar head and neck, we added additional landmarks and semi-landmarks on the condylar process (Figure 2A, A') and performed geometric morphometric analysis. On the right (extraction side), the extraction condyle separated completely from the control (Supplemental Table 1, Supplemental Figure 3D) along PC1 (50.05%) and PC2 (10.09%; Figure 2B, Supplemental Table 2). The wireframe diagram shows that the condylar head and neck were narrower in the extraction condyle compared to control (Figure 2C). In addition, the condylar head surface was more convex in the extraction model compared to control (Figure 2C). These differences are exemplified in the representative isosurfaces of the right extraction and control condyles (Figure 2C'). Similarly, the left (non-extraction) condyle significantly separated from control (Supplemental Table 1, Supplemental Figure 3E) along PC1 (50.05%) and PC2 (11.19%; Figure 2E, Supplemental Table 2), although there was more variability among the control and extraction groups since the data did not

cluster as tightly compared to the right side. We observed similar changes in the shape of the condyle on the left side as the right, with decreased condylar head and neck lengths and increased convexity at the condylar surface in the left (non-extraction) side in the experimental animals compared to control (Figure 2F, F'). In addition, linear measurements were taken to measure the condylar head and neck widths, and both the right and left condylar processes had significantly narrower condylar heads and necks compared to control (Figure 2D, G).

We also analyzed the skull (cranium, cranial base, and maxilla) to determine whether extraction of molars in the maxillary right quadrant resulted in asymmetric growth of the skull. We found there was a significant difference in the shape of the cranium between control and extraction mice (Supplemental Table 1). This shape difference appears to be primarily in the alveolar process length (distance between most mesial point of the first molar (points 30 and 31 in Supplemental Figure 1A') and most distal point of the third molar (points 32 and 33 in Supplemental Figure 1A')), however, these points were difficult to reliably landmark in the right quadrant of the experimental mice in which the molars were extracted. Thus, the biological significance of this finding is not clear, and there do not appear to be any other clear shape changes in the cranium of the experimental mice compared to control. Although we extracted at 3 weeks and allowed the mice to grow during a major growth period, it is possible that this period of time was not long enough to see changes in the skull morphology. It will be interesting to follow up on these results by examining the skulls of mice 6 months after extraction at which time there may be compensatory, asymmetric growth in the skull in response to changes in the mandibular growth.

Thus, both the right (extraction side) and left (non-extraction side) mandibles in the experimental mice differed significantly in shape compared to control. Furthermore, there were significant changes in the shape of both the right and left condylar processes in the extraction model compared to control, including narrowing of the condylar head and neck and increase in convexity of the condylar surface. These results show that the extraction of molars in the maxillary quadrant results in significant changes in the shape of the mandible and particularly in the condylar process.

The condylar process bone volume was decreased and density increased in the extraction model compared to control.

We next wanted to determine whether extraction of the maxillary molars resulted in changes in the bone volume and density of the condylar process. We hypothesized that the extraction may result in osteoarthritic type changes in which total bone volume would decrease, and bone of increased density would be deposited in the condylar process. Indeed, the total bone volume of the condylar process on the right (extraction side) was decreased by 14.86% and left (non-extraction side) by 16.17% in the extraction mice compared to control (Figure 3A, A', C, C'). This loss of bone volume further suggests degenerative changes in the condyles with extraction.

Although the total bone volume of the condylar processes in the extraction model was decreased, the bone density was increased compared to control. Renderings of the condylar processes with the color representing the relative bone mineral density show that overall, the right and left condylar processes in the extraction model had denser bone than control (Figure 3A, A'). In particular, near the condylar head surface, the bone was

denser (more green than blue) in the extraction model condyles, both right and left, compared to control (Figure 3A, A'). Quantification of the relative bone mineral density of the condylar processes confirmed that the bone mineral density of the right and left condylar processes in the extraction mice was significantly increased by 4.96% and 5.60%, respectively, compared to control (Figure 3B, B'). Of note, we also quantified the bone density in the entire skull and mandible, and there was no significant difference between extraction and control mice, and so the alterations in bone density appear to be specific to the condylar process. These data suggest there was loss of total bone volume in the condylar processes and deposition of bone of increased density near the condylar head surface in both the right and left condyles of the experimental mice compared to control.

There was an increase in maturation stage and hypertrophic chondrocytes and osteoblasts in the MCC in the extraction mice compared to control.

In order to further understand the degenerative changes in the condyle in the experimental compared to control mice at the tissue and cellular level, we completed histological analyses of the TMJ in the extraction and control model. H&E staining of coronal sections of the TMJ showed that compared to control, the MCC was thinner on both the extraction and, to a lesser extent, on the non-extraction side in the experimental mice (Figure 4A-C'). In both condyles of the mice with extractions, the width of the MCC was decreased and the cells appeared to be more tightly packed together from the superficial to deeper surface compared to control (Figure 4A'-C'). Similarly, Safranin O staining showed that the MCC (stained red) in the extraction condyle in the experimental

mice was indeed thinner than the control (Figure 5A,B). Furthermore, the staining on the experimental condyle is lighter and more diffuse compared to control suggesting a loss of proteoglycans form the remaining cartilage which are key markers of cartilage. These data show that extraction of the maxillary molars resulted in a thinning of the MCC compared to control.

We also wanted to determine whether cell proliferation or apoptosis was altered in the MCC in the extraction model compared to control. With the samples collected for this project, immunofluorescence staining with antibodies against Ki67 or PH3, both markers of proliferation, revealed very few proliferative cells in the condyle at the 6 week timepoint in both the extraction and control samples. It was not clear whether the tissue preparation (long term EDTA treatment to demineralize the samples) disrupted the antigens. We were not able to collect convincing data on the proliferation levels in the condyle, and in the future, we plan to inject additional mice with BrdU, a thymidine analog that is incorporated into the newly synthesized DNA in proliferating cells, as a more robust marker of proliferation to determine the proliferation levels in the condyle and whether there were differences in the extraction model compared to control.

We collected preliminary data on the level of apoptosis in the condylar heads of extraction and control mice using TUNEL staining. We found that while there was no significant difference in the number of TUNEL+ cells in the condylar head in the extraction side compared to control, there was a significant 52% decrease in TUNEL+ cells on the non-extraction side compared to the extraction side and control (Figure 6A-D, N=3 control and 3 extraction mice). Thus, the level of cell death was similar on the extraction side and control, however, there was a significant decrease on the non-extraction side. Further

experiments with additional samples will be necessary to confirm these preliminary data. A possible hypothesis is the altered position of the non-extraction side condyle may result in decreased force on the condyle and decreased cell death; however, additional experiments will be necessary to test this hypothesis.

Considering the alterations in the MCC in the extraction model, we wanted to further determine whether the cellular composition of the MCC was altered due to extraction. We decided to explore the levels of chondrocyte markers *Col2* and *Col10*, osteoblast and fibroblast marker *Col1*, and osteoclast activity marker *Mmp13* at the RNA level using RNA Scope, a method of *in situ* hybridization. We observed an expansion in the MCC of expression of *Col2* and *Col10* in both condyles of the experimental mice, which suggests an increase in maturation stage and hypertrophic chondrocytes, respectively, in the MCC of the condyles of the extraction mice compared to control (Figure 7A-F). Interestingly, there was a broad expansion of *Col1* expression in the extraction condyles compared to control (Figure 7G-I). *Col1* was expressed in the developing bone in the condyle, inferior to the MCC, in the control, however, in the extraction and non-extraction condyle of the extraction mice, *Col1* was expressed more broadly in the bone and in the MCC (Figure 7G-I). These data suggest there may be *Col1* which is a marker for osteoblasts and fibroblasts in the MCC and head of the condyle in the extraction mice. Finally, the expression of *Mmp13* was increased in the condylar head region, inferior to the MCC, in the condyles of the extraction mice compared to control (Figure 7J-L), suggesting increased osteoclasts and bone turnover in the condylar heads of the experimental mice compared to control. We also explored markers of less differentiated and proliferative chondrocytes, such as *Sox9* and *Runx2*, however, we did

not see differences in expression in the condyles in the extraction and control mice (data not shown). Overall, these data suggest that, in the extraction model, the chondrocytes of the MCC were further differentiated, with an increase in maturation stage and hypertrophic chondrocytes compared to control. Furthermore, there was an increase in osteoblast and osteoclast marker expression in the extraction model suggesting an increase in bone deposition and remodeling in the condylar head. However, these cell marker data do not definitely prove cell type or activity, and further work is necessary to determine differences in chondrocyte, osteoblast, and osteoclast numbers and activities in the extraction model.

Discussion

Here, we developed a model of a mandibular functional shift by extracting molars from the maxillary right quadrant in rapidly growing 3 week-old mice in order to better understand the effect of this malocclusion on the mandible and TMJ at the tissue and cellular level. We found that extraction of the maxillary right posterior teeth resulted in changes in the shape of the mandible, most strikingly in the condylar process, which was narrower at the head and neck and more convex at the condylar surface. Furthermore, in both condylar processes of the experimental group, the total bone volume was decreased in the extraction model by 15%, and there was a 5% increase in bone density compared to the control group. The MCC was thinner in the extraction model, and there was a shift to markers of more differentiated maturation stage and hypertrophic chondrocytes and an increase in osteoblast and osteoclast markers in the MCC in the extraction model, suggesting possible bone deposition and remodeling at the condylar head due to the extraction.

We believe this extraction mouse model is useful in that it models a functional shift which can be utilized to study the pathology resulting from this malocclusion, which is common in the orthodontic clinic. In addition, it is a mouse model in which a malocclusion results in derangement and osteoarthritic-like changes in the TMJ, including thinning of the MCC. There are many models of TMJ osteoarthritis including inflammatory models, caused by injection of chemical irritants such as carrageenan, ovalbumin (Denadai et al. 2009; Habu et al. 2002); monosodium isoacetate (Kapila et al. 1995), and complete Freund's adjuvant (CFA) injection (Mazzier et al. 1967), and other malocclusion models like forced mouth opening (Kaul et al. 2016) and unilateral anterior crossbite (Zhang et

al. 2013). We believe this model has the advantage in the simplicity of extraction of teeth, rather than bonded appliances (Fuentes et al. 2003; Takenobu et al. 2008; Nakano et al. 2004, Poileka et al. 1997; Poileka et al. 2000), and it more directly links malocclusion with changes in the joint. Furthermore, this model will be useful in the study of tooth hypereruption and extrusion, since we do see hypereruption of the mandibular right molars. With this model, we can look more closely at the cellular behavior in the PDL and surrounding tissue at the root of the erupting tooth and also further understand alveolar bone remodeling around the erupting teeth.

There are, however, limitations to this model. It is a rather complex system in that extraction results in many compensations in muscle attachment and bone remodeling. Further study at multiple timepoints will be necessary to understand the compensatory changes happening due to the postural change of the mandible in this model. For example, is the mandible postured forward, and if so, is the increased stretch of the masseter inducing bone deposition on the lower border of the mandible? Furthermore, we do not entirely understand the forces that are placed on the mandible and TMJ in this model on either the extraction or non-extraction sides. We hypothesize that the mandible is shifting forward and to the right, however, additional studies such as ultrasound imaging while the mouse is functioning during chewing and direct measurements on the force in the joint would clarify the function of the altered system.

A striking finding in the study were the cellular changes at the MCC with molar extraction. There was an increase in maturation stage and hypertrophic chondrocytes in the MCC, suggesting a shift towards differentiated chondrocytes. In addition, there was an expansion in expression of *Col1* in the MCC, suggesting an increase in osteoblasts or

fibroblasts. These data suggest that cells differentiate and deposit bone in the condyle in the extraction condyle at an increased level compared to control. Furthermore, there appeared to be ectopic osteoblast expression and bone deposition in MCC at the condylar surface, supported by both expression of *Col1* and increase in bone density in that region. Whether the osteoblasts are moving into the MCC or chondrocytes in the MCC are transforming into osteoblasts, as has been shown in the condyle (Jin et al. 2015), is not clear. It would be interesting to trace chondrocytes and ostetoblasts with *Col2*[CreER] or *Col1*[CreER] drivers to answer this question and better understand cellular differentiation and activity in the MCC during this process.

The deposition and remodeling of bone in a normally cartilaginous region is suggestive of osteoarthritis, and so this model may be useful in further understanding cellular and signaling changes with the development of osteoarthritis in the TMJ. Furthermore, this phenotype appears to mimic "cortication", or deposition of bone, that we see in clinical CBCTs in juvenile idiopathic arthritis (JIA) patients once the degeneration of the condyle stabilizes (Billiau et al. 2007). This process is not well understood, and if we could better understand the mechanism, in this mouse model for example, the findings could be translated to the clinic to promote cortication or "burn out" of disease or even regenerate a more physiological MCC in these patients.

Furthermore, this study is directly clinically relevant in that the extraction mouse model tested the relationship between occlusion and adaptive responses in the TMJ. The results of our study support the widely held notion that the local biomechanical-functional environment can alter the overall shape of the mandible and growth of the MCC. Our

study also showed a relationship between malocclusion and the resulting adaptative response of the TMJ.

The malocclusion which was modeled with this extraction mouse model was a mandibular shift, which can potentially cause a skeletal crossbite in patients. Skeletal crossbites, usually associated with older adolescents and adults, are characterized by mandibular lateral displacements, asymmetric mandibles, symmetric joint spaces, and no lateral shifts from centric relation to maximum intercuspation (Bishara et al. 1994). A functional crossbite, on the other hand, is characterized by an asymmetric shift of the mandible. Children in the deciduous and mixed dentition with functional unilateral crossbites also have condyles on the crossbite site positioned relatively more superiorly and posteriorly in the glenoid fossa than the condyles on the non-crossbite side. They also have asymmetric postural muscle activity with greater resting activity on the non-crossbite site (Hesse et al. 1997). In the present study, the extraction of the molars in the upper quadrant caused a lateral shift of the mandible which resulted in compensatory changes in the morphology of the condyles and the entire mandible as well as changes in bone volume and density at the condylar surface and cell composition of the MCC. Thus, our results are consistent with clinical observations in a functional shift and this mouse model may be utilized to further understand mechanisms of the compensatory response.

The question of whether malocclusion causes TMJ dysfunction is long debated and controversial one in orthodontics. The presence of mandibular shifting in posterior crossbites has been related to muscular compensations and asymmetric postural activity with potential implications to TMJ dysfunction. As to the implications of posterior

crossbites to long term TMJ dysfunction, cross sectional studies indicate that there may be some association between the presence of posterior crossbite and symptoms of TMJ dysfunction. However, no direct cause and effect relationship between the two has been established (Thilander et al. 2002; Egermark et al. 2003; Mohlin et al. 2007). Several studies suggest that the high adaptability of the TMJ structures in growing patients appears to lessen the impact of functional posterior crossbites on long-term TMJ function (De Vis et al 1984; Alarcon et al. 2000; Throckmorton et al. 2001; Tecco et al. 2010). In a systematic review of the literature from 1970 to 2009, Thilander and his colleagues found no association between signs and symptoms of TMD with posterior crossbite patterns since they found an association between TMD and posterior crossbite was reported as often as an absence of such a relationship (Thilander et al. 2012). Thus, overall, there is still not a clear consensus in the literature on whether there is a correlation between functional posterior crossbite and TMJ dysfunction, and so more studies are necessary. Our study in a mouse model suggests a correlation between changes in occlusion and morphology of the TMJ; however, further study is necessary in this model to understand the mechanism of this relationship.

There is potential to utilize this model to further understand the mechanisms of mandibular and condylar development and remodeling and MCC growth and maintenance. This work would have tremendous potential to translate to the clinic. By understanding the mechanism of MCC growth and signaling involved, for example, we may identify therapeutic targets to modulate growth. Clinically, this information may translate into increasing growth at the condyle in a class II patient with micrognathia.

There are many clinical concerns to address, and first, a fundamental understanding of the mechanisms of TMJ development and maintenance is necessary.

Conclusion

The goal of the Master's thesis work presented here was to understand the effect of a mandibular shift malocclusion on the TMJ. We generated a model of a mandibular functional shift by extracting molars from the maxillary right quadrant in 3 week old developing mice in order to better understand the effect of this malocclusion on the mandible and TMJ at the tissue and cellular level. We found that extraction resulted in changes in the shape of the mandible, most strikingly in the condylar process, which was narrower at the head and neck and more convex at the condylar surface. Furthermore, the total bone volume of the condylar process was decreased in the extraction model by 15%, and there was a 5% increase in bone density in the condylar process compared to control. The MCC was thinner in the extraction model, and there was a shift to markers of more differentiated maturation stage and hypertrophic chondrocytes and an increase in osteoblast and osteoclast markers in the MCC in the extraction model, suggesting possible bone deposition and remodeling occurred at the condylar head due to the extraction. In this model, malocclusion resulted in derangement changes of the TMJ and an osteoarthritic phenotype in this joint. Further studies are necessary to fully understand the biomechanical environment resulting in the cellular and signaling changes in the MCC, and ultimately further our understanding of the link between occlusion and TMJ disorders.

References

1. A.G Mazzier, D.M Laskin, H.R CatchpoleAdjuvant induced arthritis in the temporomandibular joint of the rat Arch Pathol Lab Med, 83 (1967), p. 543.

2. Alarcon JA, Martin C, Palma J. Effect of unilateral posterior crossbite on electromyographic activity of human masticatory muscles. Am J Orthod Dentofacial Orthop. 2000;118:328–334.

3. Benjamin M, Ralphs JR: Biology of fibrocartilage cells. Int Rev Cytol 233:1–45. Rev Cytol 233:1–45, 2004.

4. Billiau AD, Hu Y, Verdonck A, Carels C, Wouters C. Temporomandibular joint arthritis in juvenile idiopathic arthritis: prevalence, clinical and radiological signs, and relation to dentofacial morphology. *J Rheumatol*. 2007;34(9):1925-1933.

5. Bishara SE, Burkey PS, Kharouf JG. Dental and facial asymmetries: a review. Angle Orthod 64:89-98, 1994.

6. Bishara SE, Burkey PS, Kharouf JG. Dental and facial asymmetries: a review. Angle Orthod 1994;64:89-98.

7. Bookstein FL. Landmark methods for forms without landmarks: morphometrics of group differences in outline shape. Med Image Anal. 1997;1(3):225–43.

8. Bookstein, F.L. 1997a. Landmark methods for forms without landmarks: morphometrics of group differences in outline shape. Medical Image Analysis 1(3), pp. 225–243.

9. Bookstein, F.L. 1997b. Morphometric tools for landmark data: geometry and biology.Cambridge: Cambridge University.

10. Bravetti P, Membre H, El Haddioui A, Gérard H, Fyard JP, Mahler P and Gaudy JF: Histological study of the human temporo-mandibular joint and its surrounding muscles. Surg Radiol Anat 26: 371-378, 2004.

11. Cardini A, Loy A. On growth and form in the "computer era": from geometric to biological morphometrics. Virtual Morphology and Evolutionary Morphometrics in the New Millennium. Hystrix, the Italian Journal of Mammalogy. Associazione Teriologica Italiana; Rome, Italy. pp. 1–5. 2013.

12. Cevidanes L.H., Styner M.A., Proffit W.R. Image analysis and superimposition of 3-dimensional cone-beam computed tomography models. Am. J. Orthod. Dentofac. Orthop. 2006;129:611–618. doi: 10.1016/j.ajodo.2005.12.008

13. Chang, H.-P., Liu, P.-H., Tseng, Y.-C., Yang, Y.-H., Pan, C.-Y. and Chou, S.-T. 2014. Morphometric analysis of the cranial base in Asians. Odontology / the Society of the Nippon Dental University 102(1), pp. 81–88.

14. Cleall JF, BeGole EA, Chebib FS. Craniofacial morphology: a principal component analysis. Am J Orthod. 1979;75(6):650–66.

15. De VisH, De Boever JA, Epidemiologic survey of functional conditions of the masticatory system in Belgian children aged 3-6 years. Community Dent Oral Epidemiol. 1984;12:203–207.

16. Denadai-Souza A, Camargo Lde L, Ribela MT, Keeble JE, Costa SK, Muscar. MN (2009). Participation of peripheral tachykinin NK1 receptors in the carrageenan-induced inflammation of the rat temporomandibular joint. Eur J Pain 13:812-819.

17. Dimburg et al.Malocclusions in children at 3and 7 years of age—a longitudinal study. Eur J Orthod. 2013;35:131–137.

18.   Dudas M, Sridurongrit S, Nagy A, Okazaki K, Kaartinen V. Craniofacial defects in mice lacking BMP type I receptor Alk2 in neural crest cells. *Mech Dev*. 2004;121(2):173–182. doi:10.1016/j.mod.2003.12.003

19.   Egermark I, Magnusson T, Carlsson GE. A 20-year follow-up of signs and symptoms of temporomandibular disorders and malocclusions in subjects with and without orthodontic treatment in childhood. Angle Orthod. 2003;73:109–115. 136.

20.   Epker BN, Stella JP, Fish LC. Dentofacial deformities: integrated orthodontic and surgical correction. 2nd ed. St Louis: Mosby 1959-2095, 1999.

21.   Freudenthaler et al. Geometric morphometrics of different malocclusions in lateral skull radiographs. J Orofac Orthop (2017) 78:11-20.

22.   Fuentes M, Opperman L, Buschang P, Bellinger L, Carlson D, Hinton R. Lateral functional shift of the mandible: part II. Effects on gene expression in condylar cartilage. Am J Orthod Dentofacial Ortho 123:160-6, 2003.

23.   Ghislanzoni et al. 2017. Measuring 3D shape in orthodontics through geometric morphometrics. Progress in Orthodontics (2017) 18:38 DOI 10.1186/s40510-017-0194

24.   Gu S, Wei N, Yu L, Fei J and Chen Y: Shox2-deficiency leads to dysplasia and ankylosis of the temporomandibular joint in mice. Mech Dev 125: 729-742, 2008.

25.   Gu S, Wu W, Liu C, Yang L, Sun C, Ye W, Li X, Chen J, Long F and Chen Y: BMPRIA mediated signaling is essential for temporomandibular joint development in mice. PLoS One 9: e101000, 2014.

26. Gunz P, Mitteroecker P, Bookstein FL. Semilandmarks in 3D. In: Slice DE, editor. Modern morphometrics in physical anthropology developments in primatology: progress and prospects. New York: Kluwer Academic

27. Guyomarc'h P, Dutailly B, Charton J, Santos F, Desbarats P, Coqueugniot H. Anthropological facial approximation in three dimensions (AFA3D): Computer-assisted estimation of the facial morphology using geometric morphometrics. J Forensic Sci. 2014;59:1502-1516.

28. Habu M, Tominaga K, Sukedai M, Alstergren P, Ohkawara S, Kopp S, Fukuda J (2002). Immunohistochemical study of interleukin-1beta and interleukin-1 receptor antagonist in an antigen-induced arthritis of the rabbit temporomandibular joint. J Oral Pathol Med 31:45-54.

29. Hassan MG, Vargas R, Zaher AR, et al. Altering calcium and phosphorus levels in utero affects adult mouse mandibular morphology. Orthod Craniofac Res. 2019;22(Suppl. 1):113-119

30. Hesse KL, Artun J, Joondeph DR, Kennedy DB. Changes in condylar position and occlusion associated with maxillary expansion for correction of functional unilateral posterior crossbite. Am J Orthod Dentofacial Orthop 1997;111:410-8.

31. Hill CA, Sussan TE, Reeves RH, Richtsmeier JT. 2009. Complex contributions of *Ets2* to craniofacial and thymus phenotypes of trisomic "Down syndrome" mice. Am J Med Genet Part A 149A:2158–2165

32. Inman KE, Purcell P, Kume T, Trainor PA. Interaction between Foxc1 and Fgf8 during mammalian jaw patterning and in the pathogenesis of syngnathia. *PLoS Genet*. 2013;9(12):e1003949. doi:10.1371/journal.pgen.1003949

33.   Ishizaki K, Suzuki K, Mito T, Tanaka EM, Sato S. Morphologic, functional, and occlusal characterization of mandibular lateral displacement malocclusion. Am J Orthod Dentofacial Orthop 137:454.e1-9, 2010.

34.   Isotupa KP, Carlson DS, Makinen KK. Influence of asymmetric occlusal relationships and decreased maxillary width on the growth of the facial skeleton in the guinea pig. Ann Anat 1992;174:447-51.

35.   Jay GD, Torres JR, Warman ML, Laderer MC, Breuer KS. The role of lubricin in the mechanical behavior of synovial fluid. Proc Natl Acad Sci; 104:6194–9, 2007.

36.   Kapila et al. CBCT in orthodontics: assessment of treatment outcomes and indications of its use. Dentomaxillofacial Radiology (2015) 44, 29140282.

37.   Kaul R, O'Brien MH, Dutra E, Lima A, Utreja A, Yadav S. The Effect of Altered Loading on Mandibular Condylar Cartilage. *PLoS One.* 2016;11(7):e0160121. Published 2016 Jul 29. doi:10.1371/journal.pone.0160121

38.   Kendall DG. The diffusion of shape. Adv Appl Probab. 1977;9:428

39.   Kendall, D.G. 1989. A Survey of the Statistical Theory of Shape. Statist. Sci.4(2), pp. 87–99.

40.   Kenzaki K, Tsuchikawa K and Kuwahara T: An immunohistochemical study on the localization of type II collagen in the developing mouse mandibular condyle. Okajimas Folia Anat Jpn 88: 49-55, 2011.

41.   Klingenberg CP, Wetherill L, Rogers J, et al. Prenatal alcohol exposure alters the patterns of facial asymmetry. Alcohol. 2010;44(7–8):649–57.2.

42.   Klingenberg CP. Visualizations in geometric morphometrics: how to read and how to make graphs showing shape changes. Hystrix. 2013;24(1):1–10.

43. Klingenberg, C. P. 2011. MorphoJ: an integrated software package for geometric morphometrics. *Molecular Ecology Resources* **11:** 353-357

44. Klingenberg, C.P. 2010. Evolution and development of shape: integrating quantitative approaches. Nature Reviews. Genetics 11(9), pp. 623–635.

45. Klingenberg, C.P. 2011. MorphoJ: an integrated software package for geometric morphometrics. Molecular ecology resources 11(2), pp. 353–357.

46. Kurol J, Bergland L. Longitudinal study and cost-benefit analysis of the effect of early treatment of posterior crossbite in the primary dentition. Eur J Orthod 14:173-9, 1992.

47. Kutin G, Hawes R. Posterior crossbite in the deciduous and mixed dentition. Am J Orthod 56:491-504, 1959.

48. Laskin, GC.; Hylander, W. TMD's: an evidence-based approach to diagnosis and treatment. Chicago: Quintessence; 289-94, 2006.

49. Latif et al. Morphological variability in unrepaired bilateral clefs with and without cleft palate evaluated with geometric morphometrics. J Anat (2020) 236, pp 425-433.

50. Lele, S. 1991. Some Comments on Coordinate-Free and Scale-InvariantMethods in Morphometrics. American Journal of Physical Anthropology 85, pp. 407–417.

51. Lele, S. and Richtsmeier, J.T. 1995. Euclidean distance matrix analysis: confidence intervals for form and growth differences. American Journal of Physical Anthropology 98(1), pp. 73–86.

52. Li Q, Zhang M, Chen YJ, Zhou Q, Wang YJ and Liu J: Psychological stress alters microstructure of the mandibular condyle in rats. Physiol Behav 110-111: 129-139, 2013.

53. Li X, Liang W, Ye H, Weng X, Liu F and Liu X: Overexpression of Shox2 leads to congenital dysplasia of the temporomandibular joint in mice. Int J Mol Sci 15: 13135-13150, 2014.

54. Li X, Liang W, Ye H, Weng X, Liu F, Lin P and Liu X: Overexpression of Indian hedgehog partially rescues short stature homeobox 2-overexpression-associated congenital dysplasia of the temporomandibular joint in mice. Mol Med Rep 12: 4157-4164, 2015.

55. Li X, Liu H, Gu S, Liu C, Sun C, Zheng Y and Chen Y: Replacing Shox2 with human SHOX leads to congenital disc degeneration of the temporomandibular joint in mice. Cell Tissue Res 355: 345-354, 2014.

56. McIntyre, G.T. and Mossey, P.A. 2003. Size and shape measurement in contemporary cephalometrics. European Journal of Orthodontics 25(3), pp. 231–242.

57. McNamara JA. Functional adaptations in the temporomandibular joint. Dent Clin North Am 1975;19:457-7.

58. Mérida Velasco JR, Rodríguez Vázquez JF, De la Cuadra Blanco C, Campos López R, Sánchez M and Mérida Velasco JA: Development of the mandibular condylar cartilage in human specimens of 10-15 weeks' gestation. J Anat 214: 56-64, 2009.

59. Mitteroecker P, Gunz P. Advances in geometric morphometrics. Evol Biol.

60. Mohlin B, Axelsson S,etal. TMD inr elation to malocclusion and orthodontic treatment.Asystematic review. Angle Orthod. 2007;77:542–548.

61. Mori-Akiyama et al. Sox9 is required for determination of the chondrogenic cell lineage in the cranial neural crest. Proc Natl Acad Sci USA (2003) 100 (16):9360-5.

62. Nakano H, Maki K, Shibasaki Y, Miller AJ. Three-dimensional changes in the condyle during development of an asymmetrical mandible in a rat: a microcomputed tomography study. Am J Orthod Dentofacial Orthop 126:410-20, 2004.

63. Nakano H, Watahiki J, Kubota M, Maki K, Shibasaki Y, Hatcher D, et al. Micro x-ray computed tomography analysis for the evaluation of asymmetrical condylar growth in the rat. Orthod Craniofacial Res 6 (Suppl 1):168-72. 2003.

64. Nerder PH, Bakke M, Solow B. The functional shift of the mandible in unilateral posterior crossbite and the adaptation of the tempormandibular joints: a pilot study. Eur J Orthod 21:155-66, 1999.

65. Ohno S, Schmid T, Tanne Y, Kamiya T, Honda K, Ohno-Nakahara M: Expression of superficial zone protein in mandibular condyle cartilage. Osteoarthritis Cartilage 2006;14:807–13, 2006.

66. Owtad P, Park JH, Shen G, Potres Z and Darendeliler MA: The biology of TMJ growth modification: A review. J Dent Res 92: 315-321, 2013.

67. Owtad P, Potres Z, Shen G, Petocz P and Darendeliler MA: A histochemical study on condylar cartilage and glenoid fossa during mandibular advancement. Angle Orthod 81: 270-276, 2011.

68. Pavoni C, Paoloni V, Ghislanzoni LTH, Laganà G, Cozza P. Geometric morphometric analysis of the palatal morphology in children with impacted incisors: a three-dimensional evaluation. Angle Orthod. 2017;87(3):404–8.

69. Petren S, Bondemark L,Stierfeldt B. A systemic review concerning early orthodontic treatment of unilateral posterior crossbite. Angle Orthod. 2003;73:588–596.

70. Poikela A, Kantomaa T, Pirttiniemi P. Craniofacial growth after a period of unilateral masticatory function in young rabbits. Eur J Oral Sci 105:331-7, 1997.

71. Poikela A, Pirttiniemi P, Kantomaa T. Location of the glenoid fossa after a period of unilateral function in young rabbits. Eur J Orthod 22:105-12. 2000.

72. Polychronis G, Christou P, Mavragani M, Halazonetis DJ. Geometric morphometric 3D shape analysis and covariation of human mandibular and maxillary first molars. Am J Phys Anthropol. 2013;152(2):186–96.Klingenberg CP. Evolution and development of shape: integrating quantitative approaches. Nat Rev Genet. 2010;11(9):623–35

73. Polychronis G, Halazonetis DJ. Shape covariation between the craniofacial complex and first molars in humans. J Anat. 2014;225(2):220–31. 15.

74. Proffit WR, Turvey TA. Dentofacial asymmetry. In: Proffit WR, White RP Jr., editors. Surgical-orthodontic treatment, 2nd ed. St Louis: Mosby Year Book; 1991. p. 532-6.Publishers-Plenum Publishers; 2005. p. 73–98.

75. Purcell P, Joo BW, Hu JK, Tran PV, Calicchio ML, O'Connell DJ, Maas RL and Tabin CJ: Temporomandibular joint formation requires two distinct hedgehog-dependent steps. Proc Natl Acad Sci USA 106: 18297-18302, 2009.

76. Richtsmeier, J.T. and Lele, S. 1993. A coordinate-free approach to the analysis of growth patterns: models and theoretical considerations. Biological Reviews of the Cambridge Philosophical Society 68(3), pp. 381–411.

77. Ricks ML, Farrell JT, Falk DJ, Holt DW, Rees M, Carr J, Williams T, Nichols BA, Bridgewater LC, Reynolds PR: Osteoarthritis in temporomandibular joint of Col2a1 mutant mice. Arch Oral Biol 58: 1092-1099, 2013.

78. Sato S, Takamoto K, Fushima K, Akimoto S, Suzuki Y. A new orthodontic approach to mandibular lateral displacement malocclusion— importance of occlusal plane reconstruction. Dent Jpn 1989;26:81-5.

79. Severt TR, Proffit WR. The prevalence of facial asymmetry in the dentofacial deformities population at the University of North Carolina. Int J Adult Orthod Orthognath Surg 12:171-6, 1997.

80. Shibata et al. Runx2-deficient mice lack mandibular condylar cartilage and have deformed Meckel's cartilage. Anat Embryol (2004) 208:273-280.

81. Shibukawa Y, Young B, Wu C, Yamada S, Long F, Pacifici M, et al. Temporomandibular joint formation and condyle growth require Indian hedgehog signaling. Dev Dyn 236:426–34, 2207.

82. Solem, C. Utilizing three-dimensional data in orthodontic practice and research. Orthodontics and Craniofacial Research 2017;20 (Suppl.1):114-118.

83. Soydan SS, Deniz K, Uckan S, Unal AD and Tutuncu NB: Is the incidence of temporomandibular disorder increased in polycystic ovary syndrome? Br J Oral Maxillofac Surg 52: 822-826, 2014.

84. Takenobu I, Hideharu Y. Influence of extraoral lateral force loading on the

mandible in the mandibular development of growing rats. Am J Orthod Dentofacial Orthop 134:782-91, 2008.

85. Tecco S,Tete S,Festa F. Electromyographic evaluation of masticatory, neck, and muscle activity in patients with posterior crossbites. Eur J Orthod. 2010;32:747–752.

86. Tessler, A.Y., Franchi, L., McNamara, J.A. and Baccetti, T. 2011. Morphometric analysis of craniofacial features in mono- and dizygotic twins discordant for unilateral cleft lip and palate. The Angle orthodontist 81(5), pp. 878–883.

87. Thilander B, Bjerklin K. Posterior crossbite and temporo mandibular disorders (TMDs)—need for orthodontic treatment. Eur J Orthod. 2012;34:667–673.

88. Thilander B, Rubio G,et al .Prevalence of temporo- mandibular dysfunction and its association with malocclusion in children and adults—an epidemiologic study related to specified stages of dental development. Angle Orthod. 2002;72:146–154.

89. Thompson DW. On Growth and Form. Cambridge University Press, Cambridge, UK; 1917. 20.

90. Throckmorton G, Buschang P,e tal. Changes in the masticatory cycle following treatment of posterior unilateral crossbite in children. Am J Orthod Dentofacial Orthop. 2001;120:521–529.

91. Vinkka-Puhakka H and Thesleff I: Initiation of secondary cartilage in the mandible of the Syrian hamster in the absence of muscle function. Arch Oral Biol 38: 49-54, 1993.

92. Wang Y, Liu C, Rohr J, Liu H, He F, Yu J, Sun C, Li L, Gu S and Chen Y: Tissue interaction is required for glenoid fossa development during temporomandibular joint formation. Dev Dyn 240: 2466-2473, 2011.

93. Webster M, Sheets D. A practical introduction to landmark-based geometric morphometrics. Paleontol Soc Pap. 2010;16:163–88.

94. Wu Y, Gong Z, Li J, Meng Q, Fang W and Long X: The pilot study of fibrin with temporomandibular joint derived synovial stem cells in repairing TMJ disc perforation. Biomed Res Int 2014: 454021, 2014.

95. Yokohama-Tamaki T, Maeda T, Tanaka TS and Shibata S: Functional analysis of CTRP3/cartducin in Meckel's cartilage and developing condylar cartilage in the fetal mouse mandible. J Anat 218: 517-533, 2011.

96. Zhang, X, Dai, J, Lu, L, Zhang, J, Zhang, M, Wang, Y, Guo, M, Wang, X, Wang, M. 2013. Experimentally created unilateral anterior crossbite induces a degenerative ossification phenotype in mandibular condyle of growing Sprague-Dawley rats. J Oral Rehabil. 40(7):500–508. Jing Y, Zhou X, Han X, et al. Chondrocytes Directly Transform into Bone Cells in Mandibular Condyle Growth. *J Dent Res*. 2015;94(12):1668-1675.
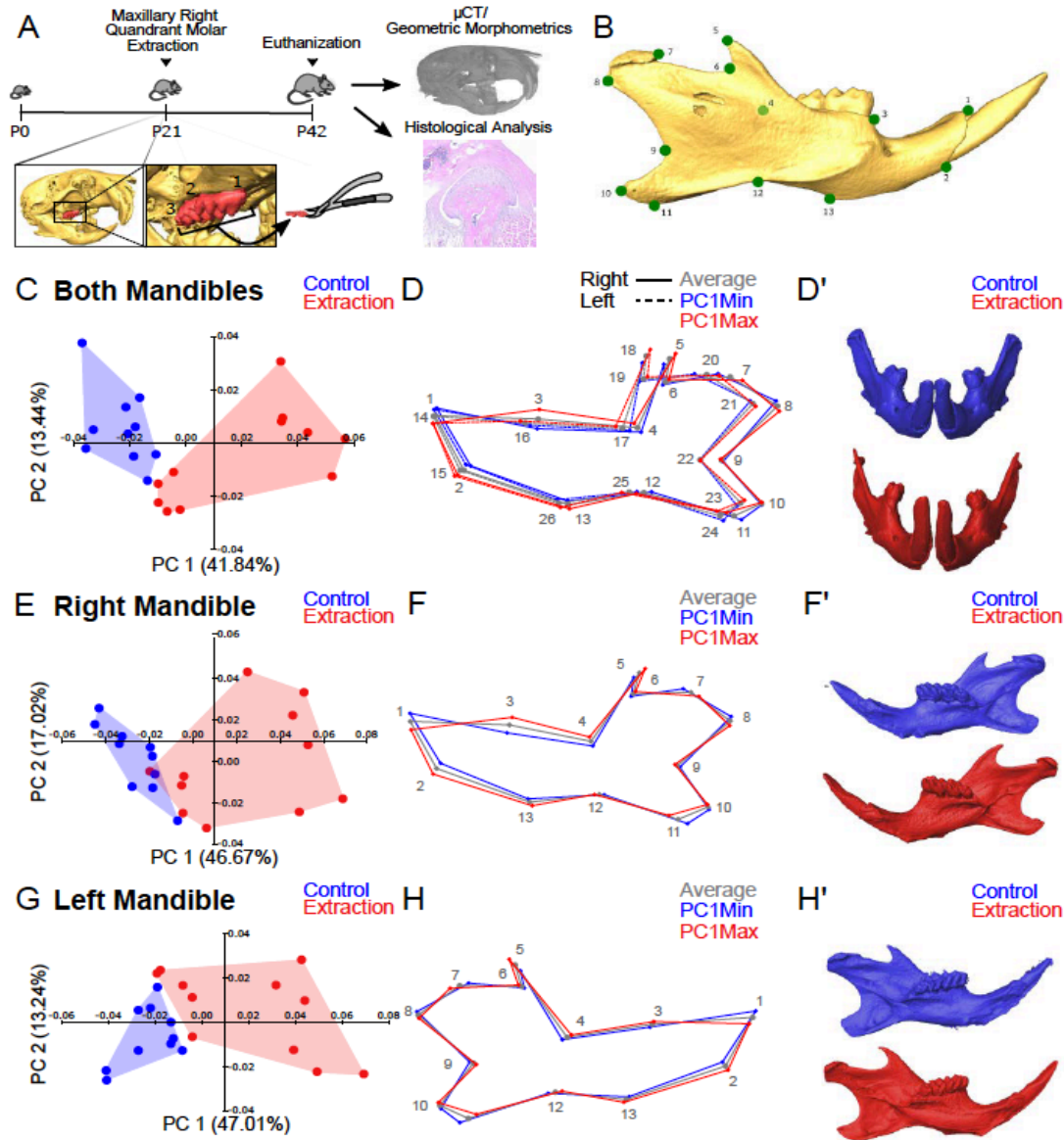
Figure 1. Extraction of maxillary right molars results in significant changes in mandibular shape. (A) Schematic of experimental design. All 3 molars were extracted from the maxillary right quadrant at postnatal day P21, and mice were euthanized for geometric morphometric and histological analysis at P42. (B) Isosurface of a hemimandible with landmarks utilized in the study. (C) Principal Component analysis (PCA) comparing both mandibles shows that the control (in blue) and extraction (in red) samples separate along PC1 and PC2. (D) Wireframes showing average (in gray), PC1 Min (in blue) PC1 Max (in red) of right (solid line) and left (dashed line) hemimandibles. (D') Representative isosurface of control and extraction mandibles. PCA (E'), wireframes (F), and isosurfaces (F') of right mandibles show increased alveolar bone height, increased height at the lower border of the mandible, decreased length of the angular process, and increased posterior-inferior tip of the condylar process in extraction samples compared to control. (G-H') Similar shape differences in the lower

53

border of the mandible, angular process, and condylar process were observed in the left mandibles of the experimental mice compared to control.
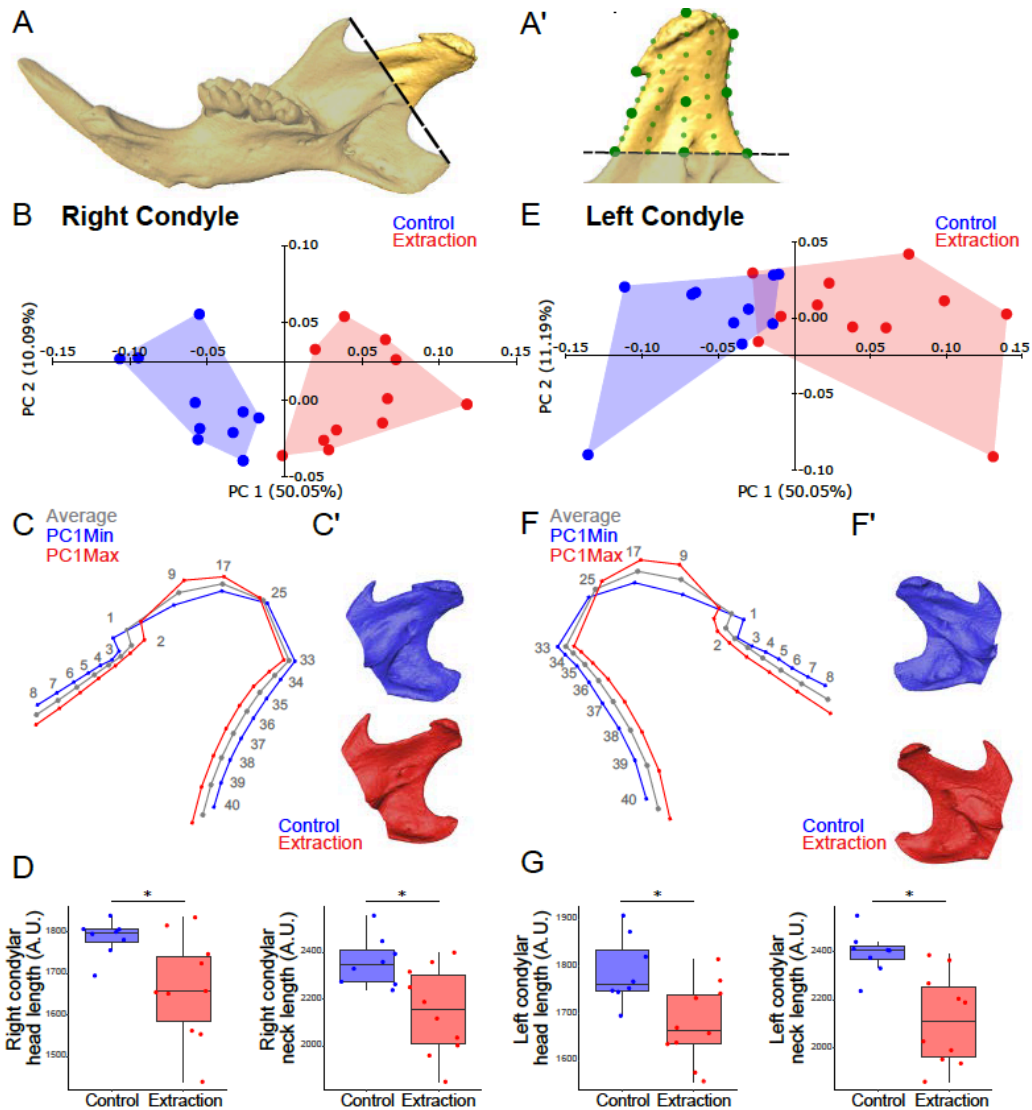
Figure 2. Extraction of maxillary right molars alters the shape of the condylar processes significantly. (A) Isosurface of a hemimandible showing region of condylar process measured (demarcated by dashed line). (A') Isosurface of condyle showing landmarks (large green dots) and semi-landmarks (small green dots) utilized. (B) Principal Component Analysis (PCA) comparing right condyles shows that the control (in blue) and extraction (in red) separate along PC1 and PC2. (C) Wireframes showing average (in gray). PC1 Min (in blue), and PC1 Max (in red) of right condyles show the extraction condylar head and neck were narrower and condylar surface more convex compared to control. (C') Representative isosurfaces of control and extraction condyles. (D) Linear measurements of right condylar width and neck lengths were decreased in extraction compared to control. PCA (E), wireframes (F), isosurfaces (F') and linear measurements (G) show left condyles were also narrower and more convex at the surfaces in extraction vs. control. *p<0.05
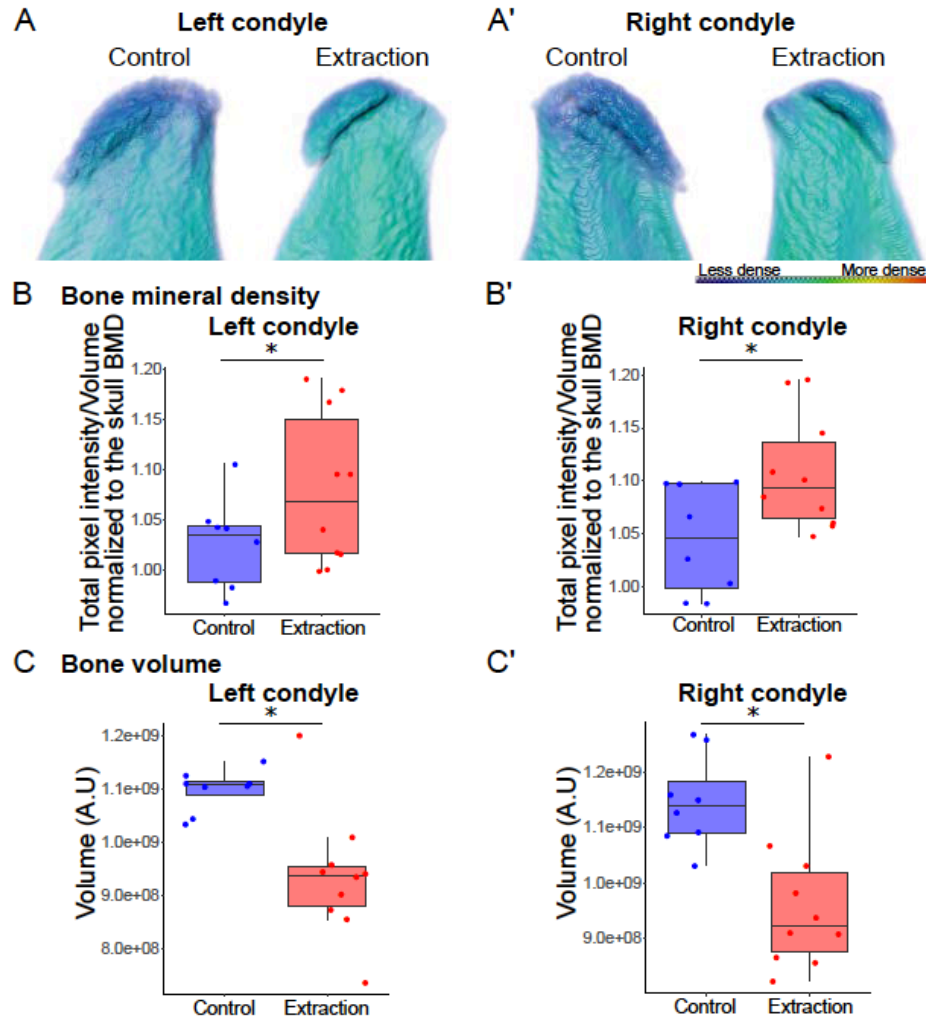
55

Figure 3. The condylar processes in the extraction model have decreased bone volume and increased bone mineral density compared to control. (A,A') Renderings of the condylar processes with the color representing the relative bone mineral density (scale: red, more dense and blue, less dense) show that the right and left condylar processes in the extraction model had decreased bone volume and increased bone density, particularly near the condylar head surface, than control. (B-C') Quantification shows a significant increase in bone mineral density of the left (B) and right (B') condylar processes in the extraction samples compared to control and significant decrease in bone volume in both the left (C) and right (C') experimental condyles compared to control. *p<0.05
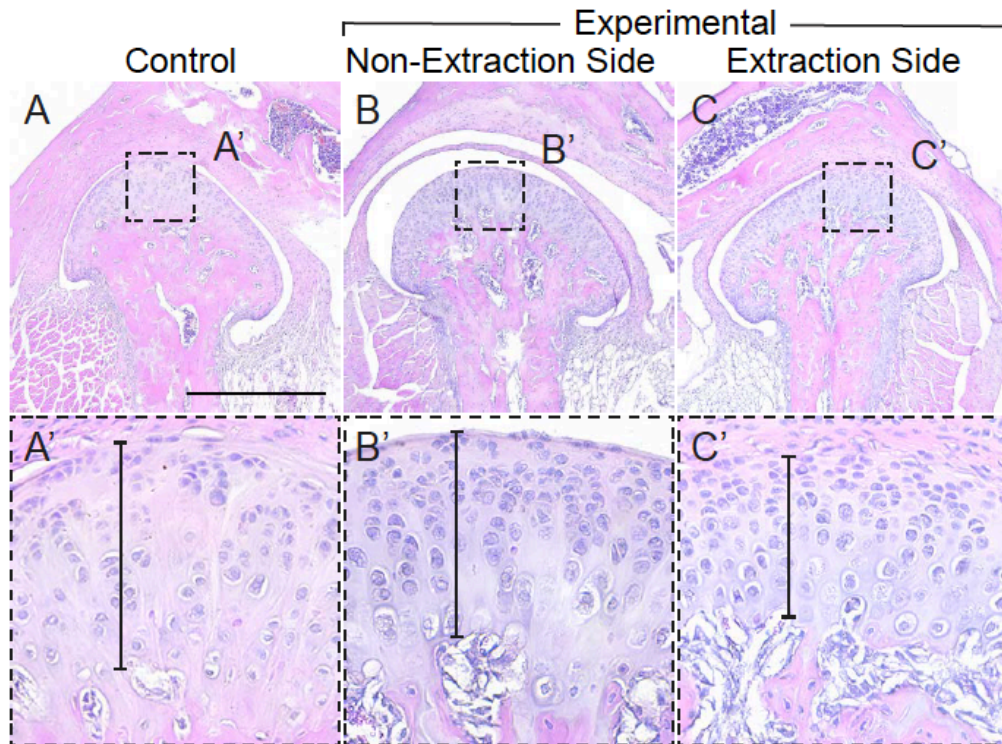
Figure 4. The mandibular condylar cartilage is thinner, and the chondrocytes appear compacted in the extraction condyle compared to control. (A-C') H&E staining shows the mandibular condylar cartilage of the non-extraction side (B,B') and extraction side (C,C') condyles in the experimental animals was thinner (demarcated by black lines) compared to control (A, A'). The chondrocytes appeared more tightly packed in the non-extraction and extraction (B,B',C,C') condyles compared to control (A,A').
Scale bar= 500μm
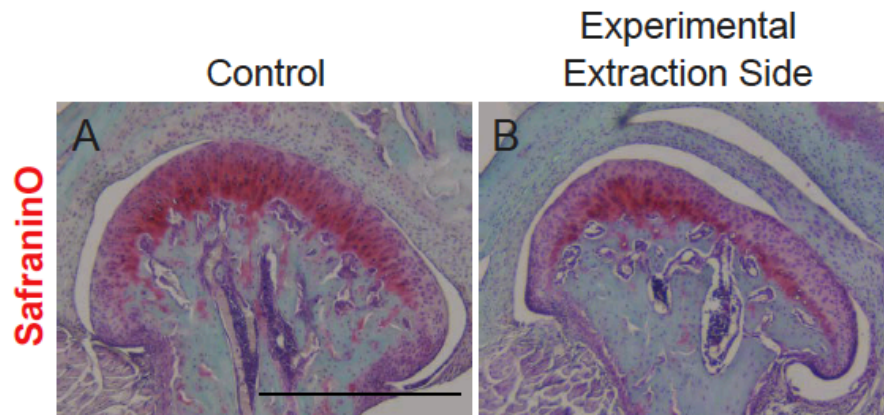
Figure 5. The mandibular condylar cartilage is thinner in the extraction condyle compared to control. (A-B) SafrarinO staining shows that the mandibular condylar cartilage was thinner in the extraction side condyle in the experimental mice (A) compared to control (B). Scale bar= 500μm
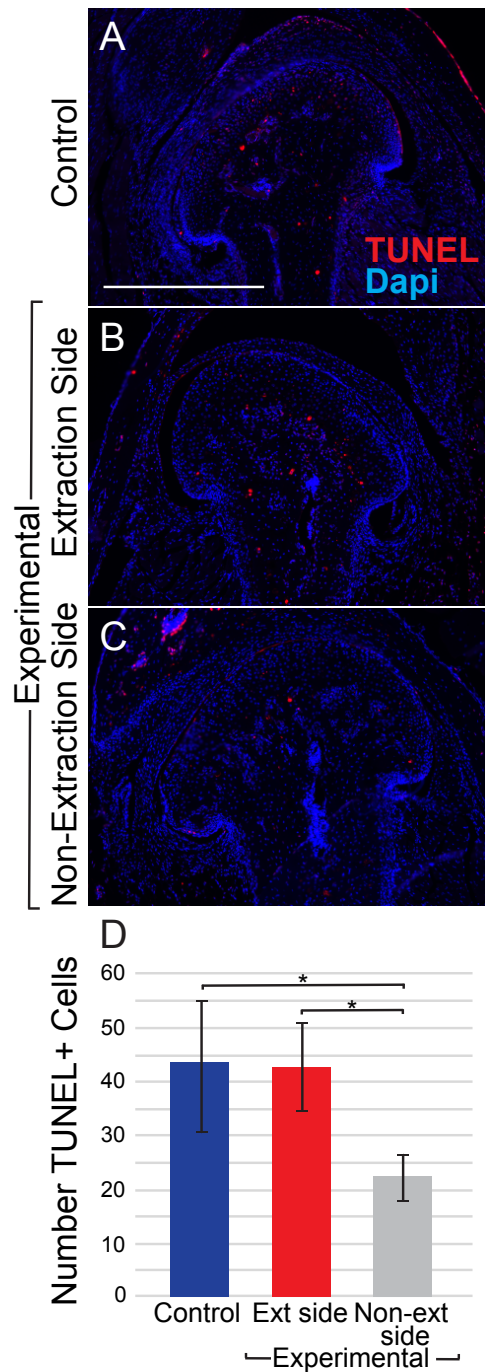
Figure 6. There is decreased apoptosis in the non-extraction side condyle compare to the extraction side and control. (A-C) TUNEL staining showed similar levels of apoptosis in the extraction side condyles in the experimental mice (B) and control (A), however, there was a significant decrease in apoptosis in the non-extraction condyle (C) in the experimental mice. (D) Quantification shows a decrease in the number of TUNEL + cells in non-extraction compared to extraction and control condyles *p<0.05.
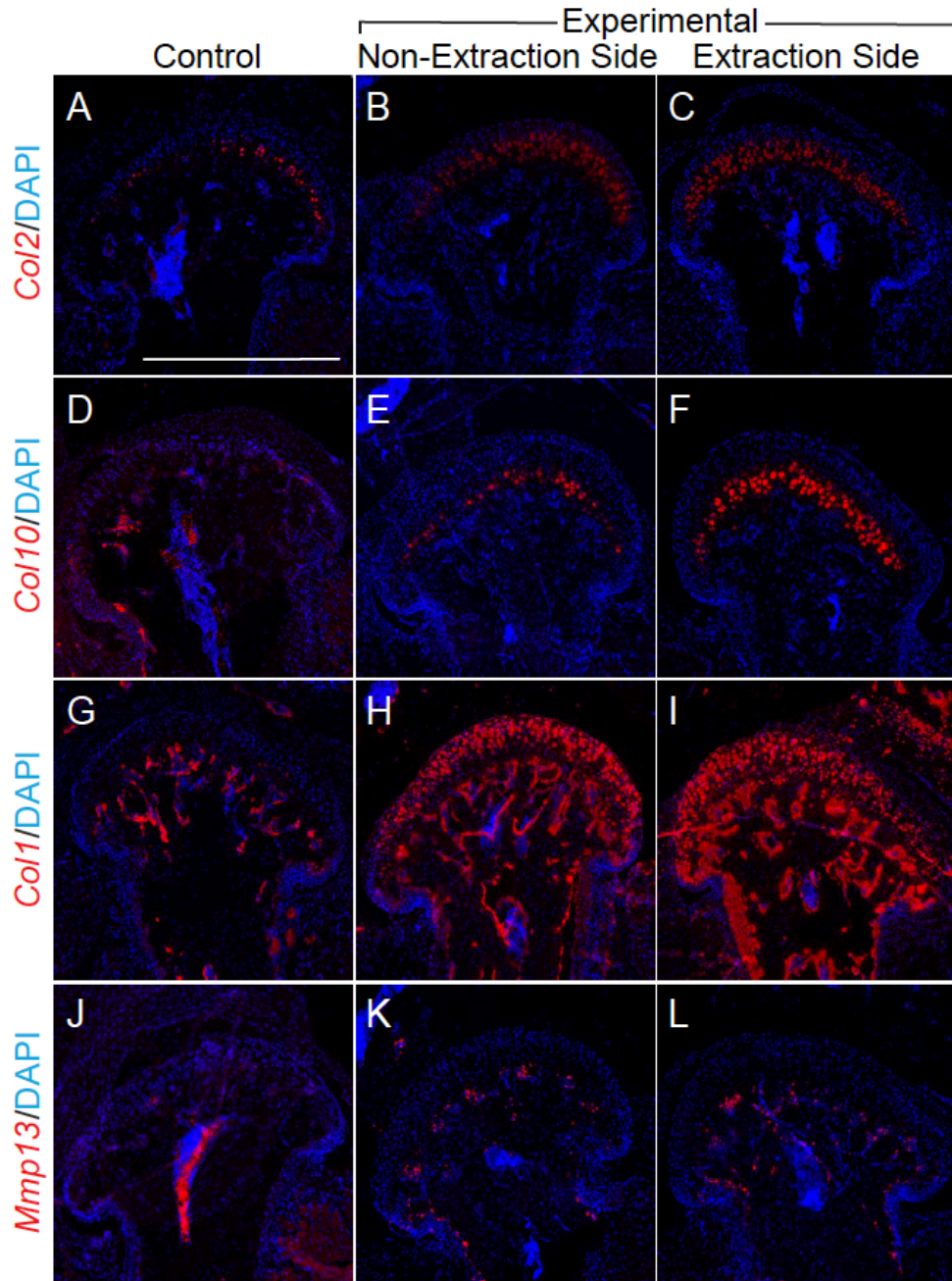Scale bar= 500μm

Figure 7. There is an increase in expression markers of maturation stage and hypertrophic chondrocytes, osteoblasts and osteoclasts in the mandibular condylar cartilage of extraction mice compared to control. (A-C) RNA scope with probe against *Col2* (red, counterstain with DAPI, blue) shows increased expression in both the non-extraction (B) and extraction (C) side mandibular condylar cartilage (MCC) compared to control (A). (D-F) Similarly, there was increased expression of *Col10* in the MCC of non-extraction (E) and extraction (F) condyles compared to control (D). (G-I) There was a striking increased in *Col1* expression in the MCC and condylar head in the extraction mice compared to control. (J-L) There was also an increase in *Mmp13* expression in the

condylar head of the non-extraction (K) and extraction (L) mice compared to control (J). Scale bar= 500μm
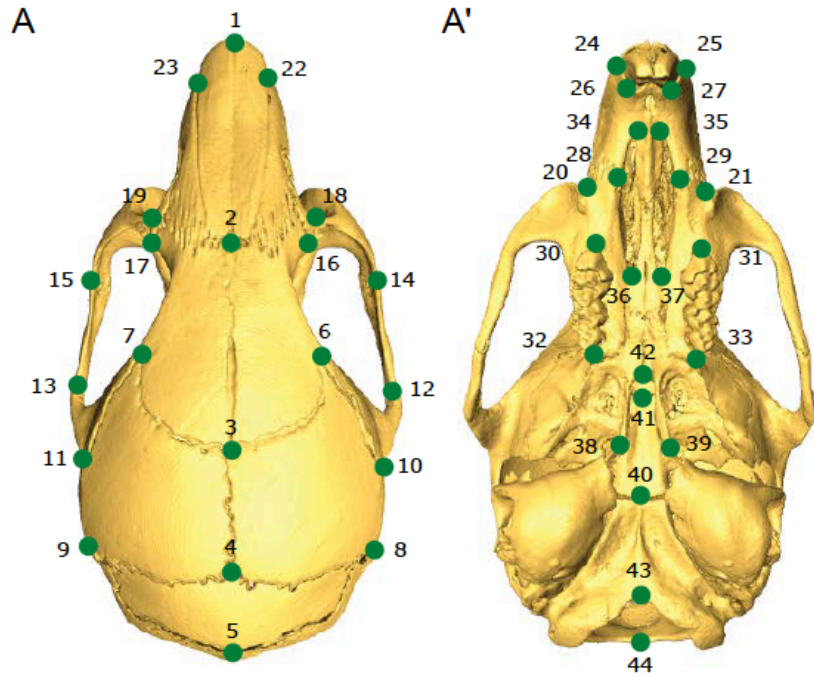
Supplemental Figure 1. Cranium landmarks. (A) Dorsal and (A') ventral views of the isosurface of the cranium with landmarks utilized for the study marked by numbered green dots
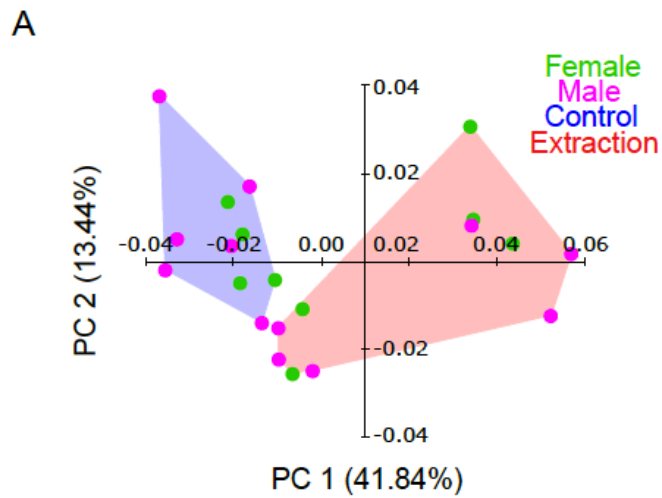
Supplemental Figure 2. No clear sex differences are observed in control or extraction samples. (A) Principal Component Analysis (PCA) showed the male and female samples did not cluster in the control or extraction groups, suggesting the shape differences observed due to extraction were significantly different between males and females.
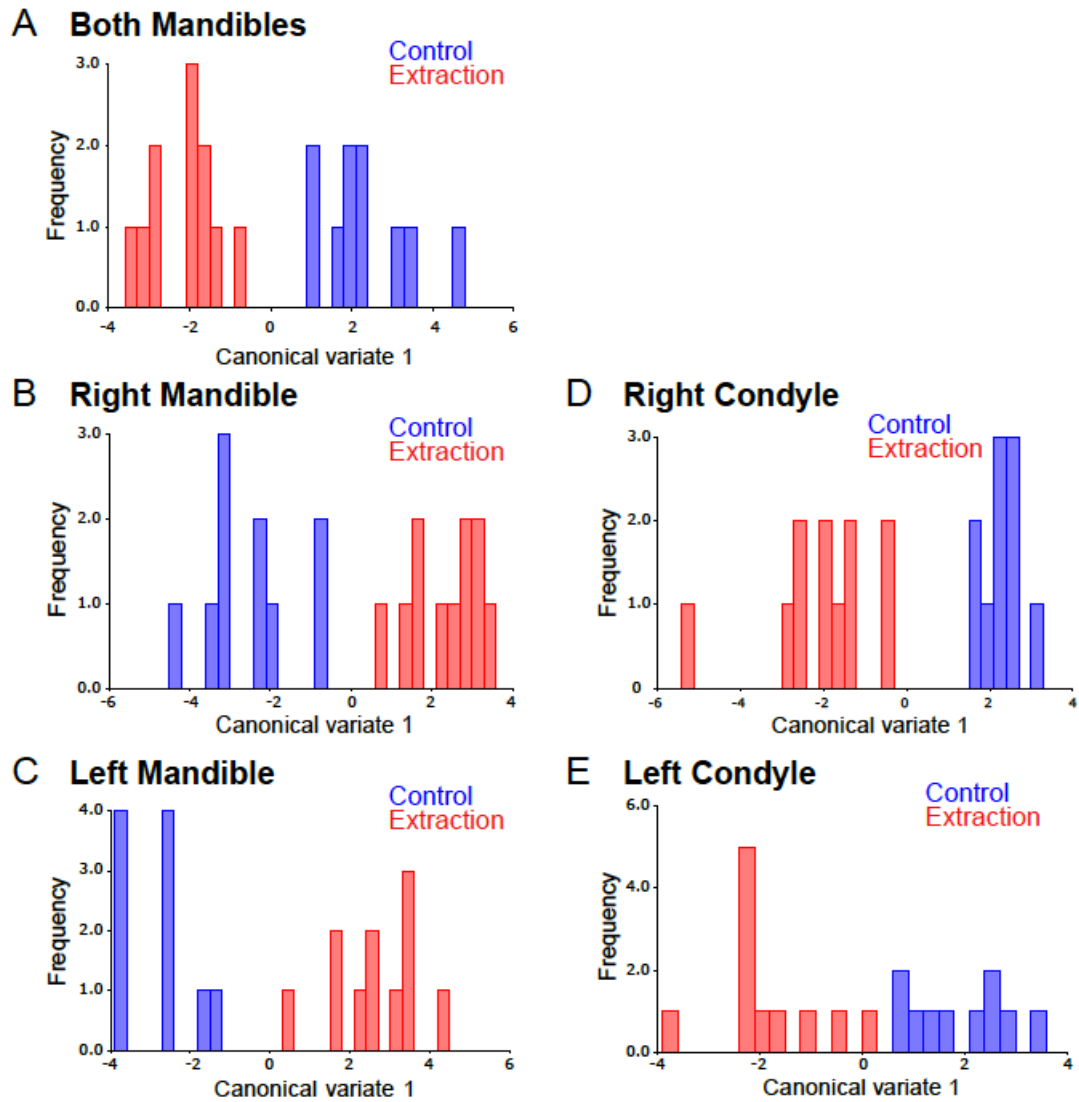
Supplemental Figure 3. Canonical variate analysis on mandibles and condyles in extraction mice compared to control. (A-C) Canonical Variate Analysis shows clear separation between both mandibles (A), the right mandible (B), the left mandible (C), the right condyle (D), and the left condyle (E) in control (blue) and extraction (red) samples.
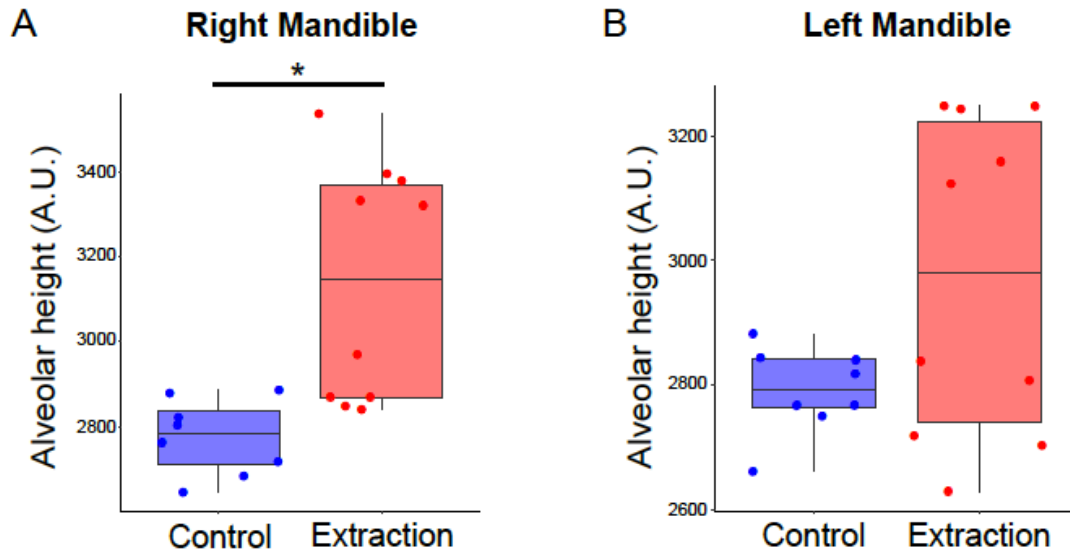
Supplemental Figure 4. The alveolar height of the right mandible in the extraction mice is significantly increased compared to control. (A) Linear measurements of the alveolar height in the right mandible showing significant increase in the extraction height in the left mandible between control and extraction mice.

Supplemental Table 1. Probability values from statistical hypothesis tests using calculated centroid size and Procrustes distance. Bold indicated p<0.05.

	p-value		
	Centroid size	Procrustes Distance	
	Control/Experiment	Control/Experiment	Male/Female
Both Mandibles	0.32748866	**<.0001**	0.4762
Right Mandible	0.268456023	**<.0001**	0.4609
Left Mandible	0.205705201	**0.0006**	0.3319
Right Condyle	0.865153994	**0.0001**	0.3548
Left Condyle	0.98617899	**0.0001**	0.382
Cranium	0.142468966	**0.0023**	0.2883

Supplemental Table 2. Contribution of each Principal Component to the shape difference of the mandibles, condyles, and cranium.

Principal Component	Variance (%)					
	Both Mandibles	Right Mandible	Left Mandible	Right Condyle	Left Condyle	Cranium
1	41.837	46.671	47.071	41.43	50.047	34.046
2	13.444	17.018	13.241	10.091	11.188	12.136
3	9.679	10.498	9.731	8.666	8.146	9.321
4	7.121	6.273	6.072	6.92	5.445	6.989
5	5.498	3.544	5.439	6.081	4.939	6.562
6	4.772	3.414	3.866	4.904	4.028	4.92
7	3.001	2.555	3.27	3.919	2.765	4.158
8	2.709	2.154	2.436	3.325	2.238	3.573
9	1.945	1.592	1.784	2.829	1.759	2.946
10	1.694	1.516	1.609	2.416	1.477	2.612
11	1.639	1.021	1.21	1.756	1.438	2.487
12	1.434	0.833	1.109	1.442	1.235	1.969
13	1.156	0.707	1.089	1.254	1.172	1.661
14	1.028	0.647	0.796	1.071	1.078	1.437
15	0.75	0.449	0.483	1.041	0.789	1.358
16	0.698	0.356	0.264	0.847	0.654	1.137
17	0.554	0.328	0.218	0.705	0.494	1.02
18	0.401	0.18	0.178	0.595	0.454	0.987
19	0.385	0.165	0.076	0.37	0.363	0.681
20	0.254	0.078	0.057	0.339	0.292	

Publishing Agreement

It is the policy of the University to encourage open access and broad distribution of all theses, dissertations, and manuscripts. The Graduate Division will facilitate the distribution of UCSF theses, dissertations, and manuscripts to the UCSF Library for open access and distribution. UCSF will make such theses, dissertations, and manuscripts accessible to the public and will take reasonable steps to preserve these works in perpetuity.

I hereby grant the non-exclusive, perpetual right to The Regents of the University of California to reproduce, publicly display, distribute, preserve, and publish copies of my thesis, dissertation, or manuscript in any form or media, now existing or later derived, including access online for teaching, research, and public service purposes.

Author Signature

6/8/2020

Date